

# Liquid-crystalline functional carbazole and naphthalene platforms†

Franck Camerel,<sup>\*a</sup> Bertrand Donnio<sup>\*b</sup> and Raymond Ziessel<sup>\*a</sup>

Received 17th June 2010, Accepted 9th September 2010

DOI: 10.1039/c0sm00547a

Two novel families of highly functionalized molecules consisting of a central carbazole or naphthalene core carrying actionable acid functions and linked to gallate platforms equipped with three long alkoxy chains have been rationally designed. The presence of amide tethers and chelating rigid fragments generate a new class of luminescent mesomorphic materials. Platforms bearing long paraffin chains ( $n = 12$  and  $16$ ) self-organize into columnar liquid crystalline phases in which the columns are arranged according to a 2D oblique, rectangular or hexagonal lattice symmetry as deduced from powder XRD experiments. FT-IR studies confirm that the common driving force for aggregation and micro-segregation in the mesophase is due to the occurrence of a tight intermolecular H-bonded network. Spectroscopic measurements show that these platforms are luminescent in solution and in the solid state. Due to the synthetic availability of carbazole and naphthalene rigid cores and the simplicity by which these platforms can be graphed, this methodology represents a practical alternative to the production of fluorescent and mesomorphic materials.

## Introduction

Over the past few years, chemists have made significant efforts in the design and synthesis of function-integrated molecules leading to soft materials with predictable and stimuli-responsive properties such as luminescence, charge transport, catalytic activity and macroscopic ordering.<sup>1</sup> A great deal of attention has been paid to the generation of self-assembled soft nanostructures originating in most cases from weak interactions (dipolar, hydrophobic, hydrogen bonding...) between preprogrammed building blocks.<sup>2</sup> Amongst these materials, liquid crystals are of particular interest since they combine order and fluidity and produce well-defined anisotropic and soft self-assembled structures from functional molecules.<sup>3</sup> For instance, discotic liquid crystals possess the ability to self-organize into ordered columnar structures and such one-dimensional assemblies offer great potential as molecular wires in electronic applications.<sup>4</sup> Due to their intriguing charge mobility, the self-assembly of  $\pi$ -conjugated molecules into linear structures has attracted much attention for its potential applications in photonics and optoelectronics devices, such as field-effect transistors (FETs),<sup>5</sup> organic light emitting diodes (OLEDs),<sup>6</sup> organic light emitting transistors (OLETs)<sup>7</sup> and solar cells.<sup>8</sup> Such one-dimensional molecular assemblies can be constructed in the solid state or in solution<sup>9</sup> through weak intermolecular hydrogen bonding,  $\pi$ - $\pi$  stacking, electrostatic, van der Waals forces and/or solvophobic interactions.

Recently, we have investigated the synthesis of functional non-discotic mesogenic platforms able to self-assemble into columnar liquid crystalline structures.<sup>10</sup> These platforms were constructed from the grafting of lipophilic gallate derivatives on central 2,6-diaminotoluene molecules functionalized by an acid function or an iodine atom in the 4-position (Chart 1). The introduction of hydrogen bonding donor-acceptor groups through the formation of amide functions was found to stabilize strongly supramolecular organisations in the solid state, in the mesomorphic state and to some extent in solution *via* aggregation processes.<sup>11</sup> The introduction of grafting sites such as an acid function or an iodine atom has allowed the introduction of various functionalities on these mesogenic platforms through the formation of ester or amide links or directly by Sonogashira cross-couplings to produce functional liquid crystalline matter.<sup>12</sup> More recently, luminescence was introduced by the grafting of organic luminophores, displaying exceptional optical properties,<sup>13</sup> or by the anchorage of platinum complexes, as triplet emitters.<sup>14</sup> Several types of chelating agents were also introduced on the platforms such as polypyridine fragments or crown ethers leading to functional metallomesogens after metal chelation.<sup>12,15</sup>

The motivation for the present work consists of the incorporation of additional functionalities, such as luminescence and charge transport properties, directly onto the mesogenic platforms, while maintaining the shape and number of amide functions and leaving the grafting site unchanged, to generate novel

<sup>a</sup>Laboratoire de Chimie Moléculaire et Spectroscopies Avancées (LCOSA, Web: <http://www-lmspc.u-strasbg.fr/lcosa>) Ecole Chimie, Polymères, Matériaux (ECPM), Université de Strasbourg-CNRS (UMR 7515), 25 rue Becquerel, F-67008 Strasbourg Cedex, France. E-mail: [fcamerel@chimie.u-strasbg.fr](mailto:fcamerel@chimie.u-strasbg.fr); [ziessel@unistra.fr](mailto:ziessel@unistra.fr)

<sup>b</sup>Institut de Physique et Chimie des Matériaux de Strasbourg (IPCMS), Université De Strasbourg-CNRS (UMR 7504), 23 rue du Loess, BP 43, F-67034 Strasbourg Cedex 2, France. E-mail: [bdonnio@ipcms.u-strasbg.fr](mailto:bdonnio@ipcms.u-strasbg.fr)

† Electronic supplementary information (ESI) available: X-ray diffractograms of the mesomorphic compounds Fig. S1-S9. See DOI: 10.1039/c0sm00547a

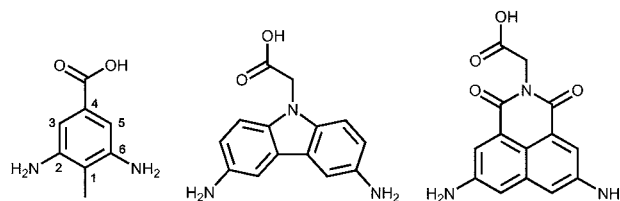


**Chart 1** Diamino molecules carrying an acid fragment at the tip used for the synthesis of functional mesogenic platforms.

families of unconventional materials able to nano-segregate and form supramolecular organized structures. For this purpose, carbazole and naphthalene derivatives have been targeted and designed to replace the central toluene core (Chart I).

Carbazole and naphthalimide molecules have both been selected as flat central cores due to the possibility of introducing two amine functions at 120° around the periphery of the core, whilst an acid function can be inserted at the tip on the nitrogen atom of the carbazole or on the imide function of the naphthalene molecule (Chart I). These two functionalized molecules were also selected for their good luminescent and charge transport properties. Carbazole-based molecules have been the subject of numerous studies in the OLED technology, essentially due to their excellent photoconductive properties and inherent electron-donating nature arising from the nitrogen atom (p type conductor). The carbazole unit is tolerant to functionalization and as such has been largely incorporated into small molecular<sup>16</sup> and macromolecular materials.<sup>17</sup> The naphthalimide moiety also displays good luminescence properties and has been extensively used as fluorescence probes for anions detection<sup>18</sup> and biological labelling.<sup>19</sup> Such  $\pi$ -conjugated aromatic fragments are also electron-deficient and can be used as n type charge carriers in optoelectronic devices.<sup>20</sup> Both skeletons are chemically robust and amenable to functionalization. Little effort has been made up to now to generate liquid crystalline materials with these building blocks.<sup>21</sup>

Herein, we report on the syntheses and thermotropic and luminescent properties of new functional mesogenic platforms with fluorescent central naphthalene or carbazole cores carrying an acid function as the grafting site and two structured lateral gallate fragments.

## Experimental

NMR Spectra (300.1 (<sup>1</sup>H) and 75.5 MHz (<sup>13</sup>C)) were recorded at room temperature using perdeuterated solvents as internal standards. FT-IR spectra were recorded using a Perkin-Elmer “spectrum one” spectrometer equipped with an ATR “diamond” apparatus. UV-vis spectra were recorded using a Shimadzu UV-3600 dual-beam grating spectrophotometer with a 1 cm quartz cell. Fluorescence spectra were recorded on a HORIBA Jobin-Yvon fluoromax 4P spectrofluorimeter with a 1 cm quartz cell for solutions or an optical fiber for solids. Temperature-dependent luminescence measurements were performed on thin films thank to the HORIBA Jobin-Yvon fluoromax 4P spectrofluorimeter equipped with an optical fiber and a heating stage (Linkam LTS350 hot-stage and a Linkam TMS94 central processor). All fluorescence spectra were corrected. The fluorescence quantum yield ( $\Phi_{\text{exp}}$ ) was calculated from eqn (1). Here,  $F$  denotes the integral of the corrected fluorescence spectrum,  $A$  is the absorbance at the excitation wavelength, and  $n$  is the refractive index of the medium. The reference system used was rhodamine 6G in methanol ( $\Phi_{\text{ref}} = 0.78$ ,  $\lambda_{\text{exc}} = 488$  nm).

$$\Phi_{\text{exp}} = \Phi_{\text{ref}} \frac{F \{1 - \exp(-A_{\text{ref}} \ln 10)\} n^2}{F_{\text{ref}} \{1 - \exp(-A \ln 10)\} n_{\text{ref}}^2} \quad (1)$$

Differential scanning calorimetry (DSC) was performed on a Netzsch DSC 200 PC/1/M/H Phox® instrument equipped with an intracooler, allowing measurements from -65 °C up to

450 °C. The samples were examined at a scanning rate of 10 K min<sup>-1</sup> by applying two heating and one cooling cycles. The apparatus was calibrated with indium (156.6 °C). Phase behaviour was studied by polarized light optical microscopy (POM) on a Leica DMLB microscope equipped with a Linkam LTS350 hot-stage and a Linkam TMS94 central processor. X-Ray scattering measurements were carried out with two different experimental set-ups. In both cases, a linear monochromatic Cu-K $\alpha_1$  beam ( $\lambda = 1.5405$  Å) was obtained using a sealed-tube generator (900W) equipped with a bent monochromator. In the first set, the transmission Guinier geometry was used, whereas a Debye-Scherrer-like geometry was used in the second experimental set-up. In all cases, Lindemann glass capillaries of 1 mm diameter and 10  $\mu$ m wall thickness were filled with the crude powder. Microwave irradiation experiments were performed using a multi-mode MARS System from CEM Corporation using standard Pyrex vessels (capacity 50 mL). The temperature profiles for microwave experiments were recorded using a fiber-optic probe protected by a sapphire immersion tube well inserted directly into the reaction mixture. Pressure profiles were recorded with a pressure sensor directly connected to the reaction vessel.

## Synthetic procedures

Syntheses of 3,4,5 trialkoxybenzoic chlorides with C<sub>12</sub> and C<sub>16</sub> chains have already been reported.<sup>22</sup>

**Compound 1.** A solution of 3,4,5-tridodecyloxybenzoic chloride (1.25 g, 1.8 mmol) in distilled THF (25 mL) was slowly added to a distilled THF solution (50 mL) containing 3,6-diaminocarbazole (0.18 g, 0.9 mmol) and triethylamine (0.5 mL, 3.6 mmol). After complete addition, the reaction mixture was stirred at room temperature under argon for 17 h. After removal of the solvent, the crude product was dissolved in dichloromethane, washed with water and dried over anhydrous MgSO<sub>4</sub>. After evaporation of the solvent, purification was performed by chromatography on alumina gel with CH<sub>2</sub>Cl<sub>2</sub>-MeOH (100/0 to 99.8/0.2) and followed by crystallization from CH<sub>2</sub>Cl<sub>2</sub>-CH<sub>3</sub>CN (0.66 g, 48%). <sup>1</sup>H NMR (CDCl<sub>3</sub>, 300 MHz)  $\delta$  0.88 (m, 18H, CH<sub>3</sub>), 0.99–1.60 (m, 108 H, CH<sub>2</sub>), 1.60–1.94 (m, 12H, CH<sub>2</sub>), 3.73–4.13 (m, 12H, OCH<sub>2</sub>), 6.91 (d, 2H, <sup>3</sup>J = 8.46 Hz), 7.23 (s, 4H), 7.28 (d, 2H, <sup>3</sup>J = 8.85 Hz), 7.57 (s, 2H), 8.37 (s, 1H), 8.57 (s, 2H) ppm. <sup>13</sup>C{<sup>1</sup>H} DEPT NMR (75.47 MHz, CDCl<sub>3</sub>)  $\delta$  14.09 (CH<sub>3</sub>), 22.70 (CH<sub>2</sub>), 26.18 (CH<sub>2</sub>), 26.22 (CH<sub>2</sub>), 29.41 (CH<sub>2</sub>), 29.49 (CH<sub>2</sub>), 29.56 (CH<sub>2</sub>), 29.73 (CH<sub>2</sub>), 29.78 (CH<sub>2</sub>), 29.81 (CH<sub>2</sub>), 30.45 (CH<sub>2</sub>), 31.96 (CH<sub>2</sub>), 69.27 (OCH<sub>2</sub>), 73.53 (OCH<sub>2</sub>), 105.91 (CH), 110.57 (CH), 113.97 (CH), 121.14 (CH), 122.91 (Cq), 129.26 (Cq), 129.76 (Cq), 137.75 (Cq), 141.13 (Cq), 153.14 (Cq), 166.21 (C=O) ppm. UV-vis (CH<sub>2</sub>Cl<sub>2</sub>, 23 °C):  $\lambda_{\text{max}}$  ( $\epsilon$ , M<sup>-1</sup> cm<sup>-1</sup>) = 259 (32750), 301 (51600). IR (ATR): 3275 ( $\nu$ NH), 2920, 2852, 1640 ( $\nu$ CO), 1578, 1530, 1490, 1467, 1441, 1425, 1381, 1337, 1221, 1115, 1002, 847, 805 cm<sup>-1</sup>. EI-MS:  $m/z$  (%) = 1510.1 (100) [M]<sup>+</sup>. Anal. calcd for C<sub>98</sub>H<sub>163</sub>N<sub>3</sub>O<sub>8</sub>: C, 77.88; H, 10.87; N, 2.78; Found C, 77.55; H, 10.53; N, 2.51.

**Compound 2.** To a distilled THF solution (50 mL) containing 3,6-diaminocarbazole (0.26 g, 1.0 mmol) and triethylamine (0.55 mL, 4.0 mmol), a solution of 3,4,5-trihexadecyloxybenzoic chloride (1.72 g, 2.0 mmol) in distilled THF (25 mL) was added

dropwise. After complete addition, the reaction mixture was stirred at room temperature under argon for 16 h. After evaporation of the solvent, the crude product was dissolved in dichloromethane, washed with water and the organic layers dried over anhydrous  $\text{MgSO}_4$ . Purification was performed by chromatography on alumina gel with  $\text{CH}_2\text{Cl}_2$ – $\text{MeOH}$  (100/0 to 99.7/0.3) and followed by crystallization from  $\text{CH}_2\text{Cl}_2$ – $\text{CH}_3\text{CN}$  (1.02 g, 55%).  $^1\text{H}$  NMR ( $\text{CDCl}_3$ , 300 MHz)  $\delta$  0.87 (m, 18H,  $\text{CH}_3$ ), 1.06–1.57 (m, 156 H,  $\text{CH}_2$ ), 1.66–1.90 (m, 12H,  $\text{CH}_2$ ), 4.01 (m, 12H,  $\text{OCH}_2$ ), 7.15 (s, 4H), 7.21 (d, 2H,  $^3J = 13.71$  Hz), 7.48 (d, 2H,  $^3J = 12.03$  Hz), 7.94 (s, 2H), 8.17 (s, 2H), 8.32 (s, 1H) ppm.  $^{13}\text{C}\{^1\text{H}\}$  DEPT NMR (75.47 MHz,  $\text{CDCl}_3$ )  $\delta$  14.11 ( $\text{CH}_3$ ), 22.70 ( $\text{CH}_2$ ), 26.20 ( $\text{CH}_2$ ), 29.40 ( $\text{CH}_2$ ), 29.47 ( $\text{CH}_2$ ), 29.55 ( $\text{CH}_2$ ), 29.70 ( $\text{CH}_2$ ), 29.77 ( $\text{CH}_2$ ), 29.78 ( $\text{CH}_2$ ), 30.44 ( $\text{CH}_2$ ), 30.90 ( $\text{CH}_2$ ), 31.95 ( $\text{CH}_2$ ), 69.30 ( $\text{OCH}_2$ ), 73.53 ( $\text{OCH}_2$ ), 105.84 (CH), 110.64 (CH), 113.85 (CH), 121.02 (CH), 123.05 (Cq), 129.42 (Cq), 129.82 (Cq), 137.75 (Cq), 141.16 (Cq), 153.16 (Cq), 166.16 (C=O) ppm. UV–vis ( $\text{CH}_2\text{Cl}_2$ , 23 °C):  $\lambda_{\text{max}}$  ( $\epsilon$ ,  $\text{M}^{-1} \text{cm}^{-1}$ ) = 259 (29800), 301 (48600). IR (ATR): 3285 ( $\nu\text{NH}$ ), 2916, 2850, 1641 ( $\nu\text{CO}$ ), 1581, 1538, 1493, 1467, 1425, 1380, 1335, 1223, 1117, 1014, 992, 953, 861, 847  $\text{cm}^{-1}$ . EI-MS:  $m/z$  (%) = 1847.1 (100) [ $\text{M}$ ] $^+$ . Anal. calcd for  $\text{C}_{122}\text{H}_{211}\text{N}_3\text{O}_8$ : C, 79.29; H, 11.51; N, 2.27; found C, 78.95; H, 11.34; N, 1.98.

**Compound 3.** 3,6-Dinitrocarbazole (0.5 g, 1.9 mmol) was stirred with sodium hydride (77.8 mg (60% in oil), 1.9 mmol) in 20 mL of freshly distilled *N,N*-dimethylformamide under argon for 30 min at room temperature before ethyl bromoacetate (0.35 mL, 1.5 equiv.) was added. The reaction mixture was stirred at room temperature for 20 h. The reaction was quenched with water and the formed precipitate triturated for 1 h. The precipitate was filtered, washed with water and dried under vacuum to yield a yellow powder (549 mg, 82%), which was used without further purification.  $^1\text{H}$  NMR ( $d_6$ -DMSO, 300 MHz)  $\delta$  1.23 (t, 3H,  $^3J = 5.25$  Hz), 4.19 (q, 2H,  $\text{CH}_2$ ,  $^3J = 5.36$  Hz), 5.56 (s, 2 H,  $\text{CH}_2$ ), 7.84 (d, 2H, CH,  $^3J = 6.81$  Hz), 8.35 (d, 2H, CH,  $^3J = 6.81$  Hz), 9.36 (s, 2H, CH) ppm.  $^{13}\text{C}\{^1\text{H}\}$  DEPT NMR (75.47 MHz,  $d_6$ -DMSO)  $\delta$  14.87 ( $\text{CH}_3$ ), 45.64 ( $\text{NCH}_2$ ), 62.38 ( $\text{OCH}_2$ ), 111.74 (CH), 119.27 (CH), 122.92 (Cq), 123.47 (CH), 142.44 (Cq), 145.75 (Cq), 168.69 (C=O) ppm. UV–vis ( $\text{CH}_2\text{Cl}_2$ , 23 °C):  $\lambda_{\text{max}}$  ( $\epsilon$ ,  $\text{M}^{-1} \text{cm}^{-1}$ ) = 267 (27125), 286 (18800), 358 (16900). IR (ATR): 3098, 2981, 2925, 2853, 1744, 1671, 1629, 1606, 1586, 1513, 1479, 1430, 1396, 1375, 1331, 1305, 1201, 1148, 1136, 1098, 1010, 910, 862, 819  $\text{cm}^{-1}$ . EI-MS:  $m/z$  (%) = 343.1 (100) [ $\text{M}$ ] $^+$ . Anal. calcd for  $\text{C}_{16}\text{H}_{13}\text{N}_3\text{O}_6$ : C, 55.98; H, 3.82; N, 12.24; found C, 55.67; H, 3.47; N, 11.87.

**Compound 4.** A mixture of *N*-(3,6-dinitro-carbazolyl)-ethyl acetate (0.5 g, 1.45 mmol), 10% palladium on carbon (250 mg, 33 wt %), methanol (100 mL) and glacial acetic acid (10 mL) was hydrogenated at atmospheric pressure under a balloon for 14 h. The mixture was filtered through a cake of celite and the methanol removed by rotary evaporation under reduced pressure. Saturated aqueous  $\text{NaHCO}_3$  solution was added to neutralize the acetic acid and the crude suspension was extracted with chloroform. The combined organic layers were washed with saturated aqueous  $\text{NaHCO}_3$  solution and dried over anhydrous  $\text{MgSO}_4$ . Evaporation of the solvent under reduced pressure yielded 0.34 g (82%) of a yellow solid, which darkens rapidly on

exposure to light and air. The crude product is extremely sensitive to air and light and was used without further purification.  $^1\text{H}$  NMR ( $d_6$ -DMSO, 300 MHz)  $\delta$  1.19 (t, 3H,  $^3J = 5.27$  Hz), 4.11 (q, 2H,  $\text{CH}_2$ ,  $^3J = 5.40$  Hz), 4.71 (br, 4H,  $\text{NH}_2$ ), 5.02 (s, 2 H,  $\text{CH}_2$ ), 7.84 (dd, 2H, CH,  $^3J = 6.40$  Hz,  $^4J = 1.51$  Hz), 7.10 (m, 4H, CH) ppm.  $^{13}\text{C}\{^1\text{H}\}$  DEPT NMR (75.47 MHz,  $d_6$ -DMSO)  $\delta$  14.96 ( $\text{CH}_3$ ), 44.99 ( $\text{NCH}_2$ ), 61.51 ( $\text{OCH}_2$ ), 104.86 (CH), 109.99 (CH), 115.48 (CH), 123.65 (Cq), 135.11 (Cq), 141.95 (Cq), 170.17 (C=O) ppm. UV–vis ( $\text{CH}_2\text{Cl}_2$ , 23 °C):  $\lambda_{\text{max}}$  ( $\epsilon$ ,  $\text{M}^{-1} \text{cm}^{-1}$ ) = 235 (24250), 319 (9100), 373 (3100). IR (ATR): 3382 ( $\nu\text{NH}$ ), 3194, 2957, 2924, 2848, 1731, 1677, 1618, 1580, 1498, 1474, 1441, 1422, 1368, 1326, 1261, 1238, 1189, 1151, 1120, 1070, 1030, 934, 869  $\text{cm}^{-1}$ . EI-MS:  $m/z$  (%) = 284.1 (100) [ $\text{M}$ ] $^+$ . Anal. calcd for  $\text{C}_{16}\text{H}_{17}\text{N}_3\text{O}_2$ : C, 67.83; H, 6.05; N, 14.83; found C, 67.57; H, 5.64; N, 14.64.

**Compound 5.** To a solution of *N*-ethyl-(3,6-diamino-carbazolyl)-acetate (0.2 g, 0.7 mmol) in 20 mL of distilled dichloromethane was added 2 equivalents of 3,4,5 tridodecyloxybenzoic chloride (0.98 g, 1.4 mmol) and 4 equivalents of triethylamine (0.4 mL, 2.8 mmol). The mixture was stirred at room temperature for 16 h. After removal of the solvent, the crude product was redissolved in dichloromethane, washed with water and dried over anhydrous  $\text{MgSO}_4$ . Purification was performed by chromatography on alumina gel with  $\text{CH}_2\text{Cl}_2$ – $\text{MeOH}$  (100/0 to 99.5/0.5) and followed by crystallization from  $\text{CH}_2\text{Cl}_2$ – $\text{CH}_3\text{CN}$  (0.53 g, 47%).  $^1\text{H}$  NMR ( $\text{CDCl}_3$ , 300 MHz)  $\delta$  0.87 (m, 18H,  $\text{CH}_3$ ), 1.13–1.42 (m, 99 H,  $\text{CH}_3 + \text{CH}_2$ ), 1.42–1.55 (m, 12H,  $\text{CH}_2$ ), 1.68–1.91 (m, 12 H,  $\text{CH}_2$ ), 4.04 (m, 12H,  $\text{OCH}_2$ ), 4.20 (q, 2H,  $^3J = 7.15$  Hz,  $\text{CH}_2$ ), 4.95 (s, 2H,  $\text{CH}_2$ ), 7.13 (s, 4H), 7.27 (d, 2H,  $^3J = 8.67$  Hz), 7.67 (dd, 2H,  $^3J = 8.67$  Hz,  $^4J = 1.89$  Hz), 7.97 (s, 2H), 8.24 (d, 2H,  $^4J = 1.86$  Hz) ppm.  $^{13}\text{C}\{^1\text{H}\}$  DEPT NMR (75.47 MHz,  $\text{CDCl}_3$ )  $\delta$  14.11 ( $\text{CH}_3$ ), 22.69 ( $\text{CH}_2$ ), 26.12 ( $\text{CH}_2$ ), 29.37 ( $\text{CH}_2$ ), 29.40 ( $\text{CH}_2$ ), 29.44 ( $\text{CH}_2$ ), 29.61 ( $\text{CH}_2$ ), 29.66 ( $\text{CH}_2$ ), 29.71 ( $\text{CH}_2$ ), 29.76 ( $\text{CH}_2$ ), 30.36 ( $\text{CH}_2$ ), 31.93 ( $\text{CH}_2$ ), 31.94 ( $\text{CH}_2$ ), 45.03 ( $\text{CH}_2$ ), 61.74 ( $\text{OCH}_2$ ), 69.46 ( $\text{OCH}_2$ ), 73.58 ( $\text{OCH}_2$ ), 105.83 (CH), 108.66 (CH), 113.17 (CH), 120.30 (CH), 123.24 (Cq), 130.09 (Cq), 130.63 (Cq), 138.42 (Cq), 141.38 (Cq), 153.26 (Cq), 165.70 (C=O), 168.32 (C=O) ppm. UV–vis ( $\text{CH}_2\text{Cl}_2$ , 23 °C):  $\lambda_{\text{max}}$  ( $\epsilon$ ,  $\text{M}^{-1} \text{cm}^{-1}$ ) = 261 (30100), 301 (45700). IR (ATR): 3299 ( $\nu\text{NH}$ ), 2921, 2852, 1741, 1641 ( $\nu\text{CO}$ ), 1582, 1535, 1489, 1467, 1426, 1378, 1335, 1311, 1208, 1113, 1072, 1025, 1004, 954, 861  $\text{cm}^{-1}$ . EI-MS:  $m/z$  (%) = 1596.2 (100) [ $\text{M}$ ] $^+$ . Anal. calcd for  $\text{C}_{102}\text{H}_{169}\text{N}_3\text{O}_{10}$ : C, 76.69; H, 10.66; N, 2.63; found C, 76.94; H, 10.93; N, 3.04.

**Compound 6.** Distilled dichloromethane (50 mL) containing 0.16 g of *N*-ethyl-(3,6-diamino-carbazolyl)-acetate (0.55 mmol), 0.95 g of 3,4,5-trihexadecyloxybenzoic chloride (2 equiv., 1.1 mmol) and 0.23 g of triethylamine (0.31 mL, 4 equiv., 2.2 mmol) was stirred for 24 h under argon. The solvent was removed and the crude product was redissolved in dichloromethane, washed with water and dried over anhydrous  $\text{MgSO}_4$ . Purification was performed by chromatography on alumina gel with  $\text{CH}_2\text{Cl}_2$ – $\text{MeOH}$  (100/0 to 99.7/0.3) and followed by crystallization from  $\text{CH}_2\text{Cl}_2$ – $\text{CH}_3\text{CN}$  (0.44 g, 40%).  $^1\text{H}$  NMR ( $\text{CDCl}_3$ , 300 MHz)  $\delta$  0.87 (m, 18H,  $\text{CH}_3$ ), 1.10–1.42 (m, 147 H,  $\text{CH}_3 + \text{CH}_2$ ), 1.42–1.63 (m, 12H,  $\text{CH}_2$ ), 1.68–1.92 (m, 12 H,  $\text{CH}_2$ ), 4.05 (m, 12H,  $\text{OCH}_2$ ), 4.20 (q, 2H,  $^3J = 7.10$  Hz,  $\text{CH}_2$ ),

4.98 (s, 2H, CH<sub>2</sub>), 7.11 (s, 4H), 7.30 (d, 2H, <sup>3</sup>J = 8.67 Hz), 7.69 (dd, 2H, <sup>3</sup>J = 8.67 Hz, <sup>4</sup>J = 1.32 Hz), 7.90 (s, 2H), 8.25 (s, 2H) ppm. <sup>13</sup>C{<sup>1</sup>H} DEPT NMR (75.47 MHz, CDCl<sub>3</sub>) δ 14.10 (CH<sub>3</sub>), 22.69 (CH<sub>2</sub>), 26.14 (CH<sub>2</sub>), 26.17 (CH<sub>2</sub>), 29.37 (CH<sub>2</sub>), 29.45 (CH<sub>2</sub>), 29.50 (CH<sub>2</sub>), 29.70 (CH<sub>2</sub>), 29.75 (CH<sub>2</sub>), 30.39 (CH<sub>2</sub>), 31.93 (CH<sub>2</sub>), 61.72 (OCH<sub>2</sub>), 69.42 (OCH<sub>2</sub>), 73.56 (OCH<sub>2</sub>), 105.95 (CH), 108.51 (CH), 113.43 (CH), 120.59 (CH), 123.09 (Cq), 129.73 (Cq), 130.47 (Cq), 138.36 (Cq), 141.36 (Cq), 153.19 (Cq), 165.88 (C=O), 168.38 (C=O). UV-vis (CH<sub>2</sub>Cl<sub>2</sub>, 23 °C): λ<sub>max</sub> (ε, M<sup>-1</sup> cm<sup>-1</sup>) = 261 (33100), 301 (50700). IR (ATR): 3303 (νNH), 2919, 2851, 1741, 1643 (νCO), 1582, 1534, 1489, 1467, 1427, 1375, 1335, 1309, 1207, 1115, 1070, 1022, 956, 859 cm<sup>-1</sup>. EI-MS: *m/z* (%) = 1933.2 (100) [M]<sup>+</sup>. Anal. calcd for C<sub>126</sub>H<sub>217</sub>N<sub>3</sub>O<sub>10</sub>: C, 78.25; H, 11.31; N, 2.17; found C, 78.72; H, 11.67; N, 2.55.

**Compound 7.** A mixture of *N*-ethyl-(3,6-bis(3,4,5-tridodecyloxybenzoylamido)-carbazoyl)-acetate (0.19 g, 0.12 mmol) and KOH (33 mg, 0.6 mmol) in 50 mL THF–H<sub>2</sub>O (90/10 v/v) was refluxed overnight. After complete consumption of the starting material, the pH of the hot mixture was adjusted to 2 with 10% v/v dilute HCl solution. After removal of the solvents, the crude product was dissolved in dichloromethane and washed with water. The organic layers were combined and dried over anhydrous MgSO<sub>4</sub>. After crystallization from a CH<sub>2</sub>Cl<sub>2</sub>–CH<sub>3</sub>CN mixture, the product was isolated in a fair yield as a white powder (0.10 g, 54%). Due to the low solubility of *N*-(3,6-bis(3,4,5-tridodecyloxybenzoylamido)-carbazoyl)-acetic acid in all common deuterated solvents, even in the presence of base, NMR experiments could not be performed. However, an esterification reaction with H<sub>2</sub>SO<sub>4</sub> in ethanol on this product led to the formation of the starting material *N*-ethyl-(3,6-bis(3,4,5-tridodecyloxybenzoylamido)-carbazoyl)-acetate. This result confirms the formation and the integrity of the platform in acid form. UV-vis (CH<sub>2</sub>Cl<sub>2</sub>, 23 °C): λ<sub>max</sub> (ε, M<sup>-1</sup> cm<sup>-1</sup>) = 260 (32000), 301 (49200). IR (ATR): 3246 (νNH), 2921, 2852, 1730, 1638 (νCO), 1583, 1536, 1491, 1467, 1426, 1387, 1337, 1261, 1213, 1193, 1116, 1013, 954, 845 cm<sup>-1</sup>. EI-MS: *m/z* (%) = 1568.2 (100) [M]<sup>+</sup>. Anal. calcd for C<sub>100</sub>H<sub>165</sub>N<sub>3</sub>O<sub>10</sub>·H<sub>2</sub>O: C, 75.66; H, 10.60; N, 2.65; found C, 75.87; H, 10.80; N, 2.87.

**Compound 8.** A mixture of *N*-ethyl-(3,6-bis(3,4,5-trihexadecyloxybenzoylamido)-carbazoyl)-acetate (0.25 g, 0.13 mmol) and KOH (36 mg, 0.65 mmol) in 50 mL THF–H<sub>2</sub>O (90/10 v/v) was refluxed overnight. After complete consumption of the starting material, the pH of the hot mixture was adjusted to 2 with 10% v/v dilute HCl solution. After removal of the solvents, the crude product was dissolved in dichloromethane and washed with water. The organic layers were combined and dried over anhydrous MgSO<sub>4</sub>. After crystallization from a CH<sub>2</sub>Cl<sub>2</sub>–CH<sub>3</sub>CN mixture, the product was isolated in a fair yield as a white powder (0.13 g, 53%). Due to the low solubility of *N*-(3,6-bis(3,4,5-trihexadecyloxybenzoylamido)-carbazoyl)-acetic acid in all common deuterated solvents, even in the presence of base, NMR experiments could not be performed. However, an esterification reaction with H<sub>2</sub>SO<sub>4</sub> in ethanol on this product led to the formation of the starting material *N*-ethyl-(3,6-bis(3,4,5-trihexadecyloxybenzoylamido)-carbazoyl)-acetate. This result confirms the formation and the integrity of the platform in acid

form. UV-vis (CH<sub>2</sub>Cl<sub>2</sub>, 23 °C): λ<sub>max</sub> (ε, M<sup>-1</sup> cm<sup>-1</sup>) = 261 (34100), 300 (47700). IR (ATR): 3259 (νNH), 2914, 2850, 1732, 1641 (νCO), 1583, 1535, 1492, 1467, 1427, 1379, 1336, 1275, 1260, 1212, 1118, 1011, 987, 954, 848 cm<sup>-1</sup>. EI-MS: *m/z* (%) = 1905.0 (100) [M]<sup>+</sup>, 1845.5 (30) [M–(CH<sub>2</sub>COOH)]<sup>+</sup>. Anal. calcd for C<sub>124</sub>H<sub>213</sub>N<sub>3</sub>O<sub>10</sub>: C, 78.14; H, 11.26; N, 2.20; Found C, 77.98; H, 11.55; N, 2.32.

**Compound 9.** 3,6-Dinitro-1,8-naphthalic anhydride (2.0 g, 6.9 mmol) and glycinioethylester hydrochloride (1.1 g, 7.6 mmol) were added to a 250 mL flask containing 70 mL of dry acetonitrile. Triethylamine (1.15 mL, 8.3 mmol) was added drop by drop to give a violet solution that was heated to 90 °C for 20 h. After cooling the solution to room temperature, the solvent was removed by rotary evaporation and the solid obtained purified by chromatography on alumina gel with CH<sub>2</sub>Cl<sub>2</sub>–MeOH (100/0 to 99.6/0.4) and followed by crystallization from hot CH<sub>3</sub>CN (1.3 g, 50%). <sup>1</sup>H NMR (d<sub>6</sub>-DMSO, 300 MHz) δ 1.23 (t, 3H, <sup>3</sup>J = 7.15 Hz), 4.19 (q, 2H, CH<sub>2</sub>, <sup>3</sup>J = 7.03 Hz), 4.88 (s, 2H, CH<sub>2</sub>), 9.12 (d, 2H, CH, <sup>4</sup>J = 2.07 Hz), 9.82 (d, 2H, CH, <sup>4</sup>J = 2.07 Hz). <sup>13</sup>C{<sup>1</sup>H} DEPT NMR (75.47 MHz, d<sub>6</sub>-DMSO) δ 14.47 (CH<sub>3</sub>), 42.12 (NCH<sub>2</sub>), 61.84 (OCH<sub>2</sub>), 124.05 (Cq), 127.02 (CH), 131.44 (Cq), 131.96 (Cq), 132.57 (CH), 147.70 (Cq), 161.87 (C=O), 167.96 (C=O). UV-vis (CH<sub>2</sub>Cl<sub>2</sub>, 23 °C): λ<sub>max</sub> (ε, M<sup>-1</sup> cm<sup>-1</sup>) = 269 (40700), 331 (7400). IR (ATR): 1758, 1716, 1666, 1614, 1595, 1553, 1533, 1435, 1418, 1405, 1377, 1347, 1337, 1244, 1211, 1174, 1119, 1064, 1019, 985, 959, 930, 908, 866, 832, 814 cm<sup>-1</sup>. EI-MS: *m/z* (%) = 373.1 (100) [M]<sup>+</sup>, 286.2 (20) [M–(CH<sub>2</sub>COOH)]<sup>+</sup>. Anal. calcd for C<sub>16</sub>H<sub>11</sub>N<sub>3</sub>O<sub>8</sub>: C, 51.48; H, 2.97; N, 11.26; found C, 51.28; H, 2.60; N, 10.82.

**Compound 10.** To a solution of *N*-ethyl-(3,6-dinitro-1,8-naphthalyl)-acetate (0.30 g, 0.8 mmol) dissolved in 25 mL of EtOH was added ammonium formate (1.0 g, 16.0 mmol) and palladium on carbon (10 w%) (60 mg, 1/10th of the mass of *N*-ethyl-(3,6-dinitro-1,8-naphthalyl)-acetate per nitro function). The mixture was heated at 120 °C with stirring for 15 min in a 50 mL reactor vessel under microwave irradiations (300 W). The crude reaction mixture was filtered hot on a glass frit to remove the Pd/C. Upon cooling, the product crystallized in ethanol as a yellow crystalline powder, which was filtered, washed with cold ethanol and dried under vacuum (0.23 g, 91%). <sup>1</sup>H NMR (d<sub>6</sub>-DMSO, 300 MHz) δ 1.20 (t, 3H, <sup>3</sup>J = 7.07 Hz), 4.15 (q, 2H, CH<sub>2</sub>, <sup>3</sup>J = 7.09 Hz), 4.74 (s, 2H, CH<sub>2</sub>), 5.72 (s, 4H, NH<sub>2</sub>), 6.97 (d, 2H, CH, <sup>4</sup>J = 2.07 Hz), 7.60 (d, 2H, CH, <sup>4</sup>J = 2.07 Hz) ppm. <sup>13</sup>C{<sup>1</sup>H} DEPT NMR (75.47 MHz, d<sub>6</sub>-DMSO) 14.49 (CH<sub>3</sub>), 41.52 (NCH<sub>2</sub>), 61.44 (OCH<sub>2</sub>), 110.54 (CH), 114.94 (Cq), 117.68 (CH), 122.21 (Cq), 136.09 (Cq), 148.16 (Cq), 164.08 (C=O), 168.64 (C=O) ppm. UV-vis (CH<sub>2</sub>Cl<sub>2</sub>, 23 °C): λ<sub>max</sub> (ε, M<sup>-1</sup> cm<sup>-1</sup>) = 250 (37800), 412 (8000). IR (ATR): 3361 (νNH), 1741, 1699, 1657, 1618, 1573, 1526, 1458, 1406, 1381, 1350, 1318, 1276, 1261, 1211, 1177, 1115, 1017, 984, 932, 871 cm<sup>-1</sup>. EI-MS: *m/z* (%) = 313.0 (100) [M]<sup>+</sup>, 226.1 (20) [M–(CH<sub>2</sub>COOH)]<sup>+</sup>. Anal. calcd for C<sub>16</sub>H<sub>15</sub>N<sub>3</sub>O<sub>4</sub>·H<sub>2</sub>O: C, 58.00; H, 5.17; N, 12.68; found: C, 57.84; H, 4.94; N, 12.43.

**Compound 11.** Dry dichloromethane (100 mL) containing 210 mg of *N*-ethyl-(3,6-diamino-1,8-naphthalyl)-acetate (0.7 mmol), 1.0 g of 3,4,5-tridodecyloxybenzoic chloride

(1.4 mmol) and 0.4 mL triethylamine (2.8 mmol) was stirred for 20 h under argon. The solvent was removed and the crude product was redissolved in dichloromethane, washed with water and dried over anhydrous  $\text{MgSO}_4$ . Purification was performed by flash chromatography on silica gel with  $\text{CH}_2\text{Cl}_2$ –MeOH (100/0 to 99/1) and followed by crystallization from  $\text{CH}_2\text{Cl}_2$ – $\text{CH}_3\text{CN}$  (0.42 g, 38%).  $^1\text{H NMR}$  ( $\text{CDCl}_3$ , 300 MHz)  $\delta$  0.87 (m, 18H,  $\text{CH}_3$ ), 1.12–1.57 (m, 111H,  $\text{CH}_2 + \text{CH}_3$ ), 1.68–1.89 (m, 12 H,  $\text{CH}_2$ ), 4.02 (m, 12H,  $\text{OCH}_2$ ), 4.23 (q,  $^3J = 7.1$  Hz, 2H,  $\text{CH}_2$ ), 4.84 (s, 2H,  $\text{CH}_2$ ), 7.21 (s, 4H), 8.20 (s, 2H), 8.23 (s, 2H), 8.81 (s, 2H) ppm.  $^{13}\text{C}\{^1\text{H}\}$  DEPT NMR (75.47 MHz,  $\text{CDCl}_3$ )  $\delta$  14.09 ( $\text{CH}_3$ ), 22.68 ( $\text{CH}_2$ ), 26.18 ( $\text{CH}_2$ ), 29.39 ( $\text{CH}_2$ ), 29.47 ( $\text{CH}_2$ ), 29.54 ( $\text{CH}_2$ ), 29.71 ( $\text{CH}_2$ ), 29.76 ( $\text{CH}_2$ ), 29.79 ( $\text{CH}_2$ ), 30.44 ( $\text{CH}_2$ ), 31.93 ( $\text{CH}_2$ ), 62.18 ( $\text{OCH}_2$ ), 69.44 ( $\text{OCH}_2$ ), 73.55 ( $\text{OCH}_2$ ), 103.53 (Cq), 106.13 (CH), 121.48 (Cq), 121.67 (Cq), 123.03 (CH), 123.53 (CH), 128.98 (Cq), 137.00 (Cq), 141.82 (Cq), 153.28 (Cq), 162.94 (C=O), 166.42 (C=O), 169.34 (C=O) ppm. UV–vis ( $\text{CH}_2\text{Cl}_2$ , 23 °C):  $\lambda_{\text{max}}$  ( $\epsilon$ ,  $\text{M}^{-1} \text{cm}^{-1}$ ) = 278 (59400), 291 (60000), 376 (12800), 388 (12600). IR (ATR): 3336 ( $\nu\text{NH}$ ), 2921, 2852, 1709, 1655 ( $\nu\text{CO}$ ), 1629, 1582, 1548, 1537, 1498, 1467, 1398, 1378, 1333, 1266, 1217, 1177, 1115, 1023, 933, 899, 867, 802  $\text{cm}^{-1}$ . MS (FAB+, *m*NBA): *m/z* (%) = 1626.3 (100) [*M*] $^+$ . Anal. calcd for  $\text{C}_{102}\text{H}_{167}\text{N}_3\text{O}_{12}$ : C, 75.28; H, 10.34; N, 2.58; found: C, 75.54; H, 10.66; N, 3.17.

**Compound 12.** To a solution of *N*-ethyl-(3,6-diamino-1,8-naphthalyl)-acetate (0.16 g, 0.5 mmol) in 50 mL of distilled dichloromethane was added 2 equivalents of 3,4,5-trihexadecyloxybenzoic chloride (0.86 g, 1.0 mmol) and 4 equivalents of triethylamine (0.28 mL, 2.0 mmol). The mixture was stirred at room temperature for 16 h. After removal of the solvent, the crude product was redissolved in dichloromethane, washed with water and dried over anhydrous  $\text{MgSO}_4$ . Purification was performed by flash chromatography on silica gel with  $\text{CH}_2\text{Cl}_2$ –MeOH (100/0 to 99/1) and followed by crystallization from  $\text{CH}_2\text{Cl}_2$ – $\text{CH}_3\text{CN}$  (0.34 g, 34%).  $^1\text{H NMR}$  ( $\text{CDCl}_3$ , 300 MHz)  $\delta$  0.87 (m, 18H,  $\text{CH}_3$ ), 1.10–1.57 (m, 159H,  $\text{CH}_2 + \text{CH}_3$ ), 1.69–1.89 (m, 12 H,  $\text{CH}_2$ ), 4.02 (m, 12H,  $\text{OCH}_2$ ), 4.24 (q,  $^3J = 7.15$  Hz, 2H,  $\text{CH}_2$ ), 4.85 (s, 2H,  $\text{CH}_2$ ), 7.21 (s, 4H), 8.22 (s, 2H), 8.27 (s, 2H), 8.76 (s, 2H) ppm.  $^{13}\text{C}\{^1\text{H}\}$  DEPT NMR (75.47 MHz,  $\text{CDCl}_3$ )  $\delta$  14.09 ( $\text{CH}_3$ ), 22.68 ( $\text{CH}_2$ ), 26.19 ( $\text{CH}_2$ ), 29.37 ( $\text{CH}_2$ ), 29.47 ( $\text{CH}_2$ ), 29.55 ( $\text{CH}_2$ ), 29.68 ( $\text{CH}_2$ ), 29.74 ( $\text{CH}_2$ ), 29.77 ( $\text{CH}_2$ ), 30.43 ( $\text{CH}_2$ ), 31.93 ( $\text{CH}_2$ ), 62.14 ( $\text{OCH}_2$ ), 69.46 ( $\text{OCH}_2$ ), 73.56 ( $\text{OCH}_2$ ), 103.80 (Cq), 106.12 (CH), 121.54 (Cq), 121.75 (Cq), 123.57 (CH), 124.25 (CH), 128.98 (Cq), 137.03 (Cq), 141.83 (Cq), 153.30 (Cq), 162.98 (C=O), 166.40 (C=O), 169.28 (C=O) ppm. UV–vis ( $\text{CH}_2\text{Cl}_2$ , 23 °C):  $\lambda_{\text{max}}$  ( $\epsilon$ ,  $\text{M}^{-1} \text{cm}^{-1}$ ) = 277 (54300), 290 (54400), 376 (11200), 388 (10800). IR (ATR): 3336 ( $\nu\text{NH}$ ), 2920, 2852, 1709, 1651 ( $\nu\text{CO}$ ), 1628, 1583, 1547, 1497, 1467, 1394, 1377, 1264, 1217, 1177, 1116, 1022, 933, 902, 869  $\text{cm}^{-1}$ . EI-MS: *m/z* (%) = 1963.0 (100) [*M*] $^+$ . Anal. calcd for  $\text{C}_{126}\text{H}_{215}\text{N}_3\text{O}_{12}$ : C, 77.05; H, 11.03; N, 2.14; found C, 77.34; H, 11.54; N, 2.27.

**Compound 13.** A mixture of *N*-ethyl-(3,6-bis(3,4,5-tridodecyloxybenzoylamido)-1,8-naphthalyl)-acetate (0.15 g, 0.09 mmol) and KOH (25 mg, 0.45 mmol) in 50 mL THF– $\text{H}_2\text{O}$  (90/10 v/v) was refluxed overnight. After complete consumption of the starting material, the pH of the hot mixture was adjusted to 2 with 10% v/v dilute HCl solution. After cooling to room

temperature, removal of the THF led to the precipitation of the product. The white powder obtained was washed with water, dried and recrystallized from  $\text{CH}_2\text{Cl}_2$ – $\text{CH}_3\text{CN}$  (0.13 g, 88%). Due to the low solubility of *N*-ethyl-(3,6-bis(3,4,5-tridodecyloxybenzoylamido)-1,8-naphthalyl)-acetic acid, only  $^1\text{H NMR}$  experiments could have been performed in  $\text{CDCl}_3$  in the presence of deuterated methanol.  $^1\text{H NMR}$  ( $\text{CDCl}_3 + \text{MeOD}$ , 300 MHz)  $\delta$  0.67 (m, 18H,  $\text{CH}_3$ ), 0.93–1.24 (m, 96H,  $\text{CH}_2$ ), 1.24–1.40 (m, 12 H,  $\text{CH}_2$ ), 1.48–1.73 (m, 12 H,  $\text{CH}_2$ ), 3.88 (m, 12H,  $\text{OCH}_2$ ), 4.70 (s, 2H,  $\text{CH}_2$ ), 7.10 (s, 4H), 8.29 (d, 2H,  $^4J = 1.89$  Hz), 8.47 (d, 2H,  $^4J = 1.86$  Hz). The disappearance of the quadruplet around 4.2 ppm ( $\text{CH}_2$  of the ethyl function) is a clear sign of the efficiency of the saponification. Due to the presence of methanol, the amide functions are not visible in the  $^1\text{H NMR}$  spectrum. UV–vis ( $\text{CH}_2\text{Cl}_2$ , 23 °C):  $\lambda_{\text{max}}$  ( $\epsilon$ ,  $\text{M}^{-1} \text{cm}^{-1}$ ) = 278 (60800), 290 (60600), 378 (13500), 388 (13200). IR (ATR): 3303 ( $\nu\text{NH}$ ), 2921, 2852, 1706, 1650 ( $\nu\text{CO}$ ), 1582, 1546, 1517, 1495, 1467, 1426, 1389, 1377, 1333, 1292, 1220, 1180, 1114, 1003, 934, 904, 854  $\text{cm}^{-1}$ . Anal. calcd for  $\text{C}_{100}\text{H}_{163}\text{N}_3\text{O}_{12}$ : C, 75.10; H, 10.27; N, 2.63; found C, 75.38; H, 10.29; N, 2.72.

**Compound 14.** A mixture of *N*-ethyl-(3,6-bis(3,4,5-tridodecyloxybenzoylamido)-1,8-naphthalyl)-acetate (0.25 g, 0.12 mmol) and KOH (34 mg, 0.60 mmol) in 50 mL THF– $\text{H}_2\text{O}$  (90/10 v/v) was refluxed overnight. After complete consumption of the starting material, the pH of the hot mixture was adjusted to 2 with 10% v/v dilute HCl solution. After cooling to room temperature, removal of the THF led to the precipitation of the product. The white powder obtained was filtered, washed with water, dried and recrystallized from  $\text{CH}_2\text{Cl}_2$ – $\text{CH}_3\text{CN}$  (0.20 g, 82%). Due to the low solubility of *N*-(3,6-bis(3,4,5-trihexadecyloxybenzoylamido)-1,8-naphthalyl)-acetic acid, only  $^1\text{H NMR}$  experiments could be performed in  $\text{CDCl}_3$  in the presence of deuterated methanol.  $^1\text{H NMR}$  ( $\text{CDCl}_3 + \text{MeOD}$ , 300 MHz)  $\delta$  0.66 (m, 18H,  $\text{CH}_3$ ), 0.89–1.23 (m, 144H,  $\text{CH}_2$ ), 1.23–1.41 (m, 12 H,  $\text{CH}_2$ ), 1.48–1.73 (m, 12 H,  $\text{CH}_2$ ), 3.87 (m, 12H,  $\text{OCH}_2$ ), 4.69 (s, 2H,  $\text{CH}_2$ ), 7.08 (s, 4H), 8.30 (d, 2H,  $^4J = 1.86$  Hz), 8.50 (d, 2H,  $^4J = 1.68$  Hz). The disappearance of the quadruplet around 4.2 ppm ( $\text{CH}_2$  of the ethyl function) is a clear sign of the efficiency of the saponification. Due to the presence of methanol, the amide functions are not visible in the  $^1\text{H NMR}$  spectrum. UV–vis ( $\text{CH}_2\text{Cl}_2$ , 23 °C):  $\lambda_{\text{max}}$  ( $\epsilon$ ,  $\text{M}^{-1} \text{cm}^{-1}$ ) = 278 (53350), 290 (53500), 378 (13600), 388 (13400). IR (ATR): 3303 ( $\nu\text{NH}$ ), 2918, 2850, 1707, 1657 ( $\nu\text{CO}$ ), 1582, 1548, 1517, 1496, 1467, 1426, 1392, 1378, 1333, 1288, 1221, 1179, 1116, 987, 934, 904, 854  $\text{cm}^{-1}$ . Anal. calcd for  $\text{C}_{124}\text{H}_{211}\text{N}_3\text{O}_{12}$ : C, 76.93; H, 10.99; N, 2.17; found C, 77.18; H, 11.37; N, 2.54.

**Compound 15.** *N*-(3,6-Bis(3,4,5-trihexadecyloxybenzoylamido)-1,8-naphthalyl)-acetic acid (0.13 g, 0.07 mmol) and dimethylaminopyridine (DMAP) (17 mg, 0.14 mmol) were introduced in 50 mL of distilled  $\text{CH}_2\text{Cl}_2$  in a Schlenk flask under argon. The mixture was stirred until complete solubilisation of the acid. Finally 1-[3-(dimethyl-amino)propyl]-3-ethylcarbodiimide hydrochloride (EDCI) (27 mg, 0.14 mmol) and ethylenediamine (840 mg, 14 mmol) were added to the clear solution which was stirred overnight. The solvent was removed and the crude product was redissolved in dichloromethane, washed with water and dried over anhydrous  $\text{MgSO}_4$ .

Purification was performed by crystallization from  $\text{CH}_2\text{Cl}_2$ – $\text{CH}_3\text{CN}$  (0.11 g, 81%).  $^1\text{H}$  NMR ( $\text{CDCl}_3$  + MeOD, 300 MHz)  $\delta$  0.74 (m, 18H,  $\text{CH}_3$ ), 0.97–1.30 (m, 144 H,  $\text{CH}_2$ ), 1.30–1.46 (m, 12 H,  $\text{CH}_2$ ), 1.56–1.79 (m, 12 H,  $\text{CH}_2$ ), 2.74 (s, 2H,  $\text{CH}_2$  ethylamino), 3.58 (s, 2H,  $\text{CH}_2$  ethylamino), 3.95 (m, 12 H,  $\text{OCH}_2$ ), 4.73 (s, 2H,  $\text{CH}_2$ ), 7.15 (s, 4H, CH), 8.39 (s, 2 H, CH), 8.67 (s, 2 H, CH) ppm. Due to the presence of methanol, the amide and amine functions are not visible in the  $^1\text{H}$  NMR spectrum.  $^{13}\text{C}\{^1\text{H}\}$  NMR (75.47 MHz,  $\text{CDCl}_3$  + MeOD, 50 °C)  $\delta$  13.67, 22.45, 26.00, 26.07, 29.15, 29.37, 29.43, 29.60, 30.27, 31.75, 69.50, 73.57, 106.75, 108.58, 121.87, 122.14, 122.22, 123.39, 124.18, 129.00, 132.90, 137.69, 137.78, 141.83, 153.06, 163.85, 166.79 ppm. UV–vis ( $\text{CH}_2\text{Cl}_2$ , 23 °C):  $\lambda_{\text{max}}$  ( $\epsilon$ ,  $\text{M}^{-1}\text{cm}^{-1}$ ) = 279 (52700), 289 (53100), 376 (12100), 388 (11700). IR (ATR): 3235 ( $\nu\text{NH}$ ), 2919, 2850, 1698, 1648 ( $\nu\text{CO}$ ), 1584, 1525, 1497, 1467, 1426, 1379, 1335, 1220, 1179, 1115, 984, 938, 899, 857, 804  $\text{cm}^{-1}$ . EI-MS:  $m/z$  (%) = 1978.2 (100) [M]<sup>+</sup>. Anal. calcd for  $\text{C}_{126}\text{H}_{217}\text{N}_5\text{O}_{11}$ : C, 76.51; H, 11.06; N, 3.54; found C, 76.34; H, 11.07; N, 3.57.

**Compound 16.** *N*-(3,6-Bis(3,4,5-trihexadecyloxybenzoylamido)-carbazoyl)-acetic acid (86 mg, 0.045 mmol) and dimethylaminopyridine (DMAP) (11 mg, 0.09 mmol) were introduced into 20 mL of distilled  $\text{CH}_2\text{Cl}_2$  in a Schlenk flask under argon. The mixture was stirred until complete solubilisation of the acid. Finally 1-[3-(dimethyl-amino)propyl]-3-ethylcarbodiimide hydrochloride (EDCI) (17 mg, 0.09 mmol) and *N*-(2-aminoethyl)-(3,6-bis(3,4,5-trihexadecyloxybenzoylamido)-1,8-naphthalyl)-acetamide (51 mg, 0.03 mmol) were added to the clear solution which was stirred overnight. The solvent was removed and the crude product was redissolved in dichloromethane, washed with water and dried over anhydrous  $\text{MgSO}_4$ . Purification of the product was performed by chromatography on alumina gel with  $\text{CH}_2\text{Cl}_2$ –MeOH (100/0 to 95/5) and followed by crystallization from  $\text{CH}_2\text{Cl}_2$ – $\text{CH}_3\text{CN}$  (53 mg, 53%).  $^1\text{H}$  NMR ( $\text{CDCl}_3$  + MeOD, 300 MHz)  $\delta$  0.84 (m, 36 H,  $\text{CH}_3$ ), 0.95–1.60 (m, 312 H,  $\text{CH}_2$ ), 1.62–1.90 (m, 24 H,  $\text{CH}_2$ ), 2.63 (s, 4 H,  $\text{CH}_2$ ), 4.03 (m, 24 H,  $\text{OCH}_2$ ), 5.30 (s, 4 H,  $\text{CH}_2$ ), 7.05–7.36 (m, 10 H, CH), 7.44 (s, 2 H, CH), 7.48–7.73 (m, 2 H, CH), 8.05–8.23 (m, 2 H, CH), 8.50 (s, 2 H, CH) ppm. Due to the presence of methanol, the amide and amine functions are not visible in the  $^1\text{H}$  NMR spectrum.  $^{13}\text{C}\{^1\text{H}\}$  NMR (75.47 MHz,  $\text{CDCl}_3$  + MeOD) 13.90, 22.59, 26.04, 26.10, 29.29, 29.39, 30.26, 31.85, 69.29, 73.62, 106.07, 106.33, 108.43, 110.72, 113.53, 120.95, 121.53, 122.92, 123.04, 123.55, 124.58, 128.97, 129.59, 129.95, 137.77, 137.91, 138.30, 140.93, 141.10, 141.38, 152.97, 153.00, 163.77, 166.71, 166.95 ppm. UV–vis ( $\text{CH}_2\text{Cl}_2$ , 23 °C):  $\lambda_{\text{max}}$  ( $\epsilon$ ,  $\text{M}^{-1}\text{cm}^{-1}$ ) = 298 (100500), 388 (7700). IR (ATR): 3298 ( $\nu\text{NH}$ ), 2918, 2850, 1702, 1651 ( $\nu\text{CO}$ ), 1582, 1533, 1497, 1467, 1426, 1379, 1334, 1273, 1261, 1220, 1116, 1034, 1013, 987, 951, 897, 855  $\text{cm}^{-1}$ . Anal. calcd for  $\text{C}_{250}\text{H}_{428}\text{N}_8\text{O}_{20}$ : C, 77.67; H, 11.16; N, 2.90; found: C, 78.04; H, 11.26; N, 3.17.

## Results and discussion

### Synthesis and characterisation

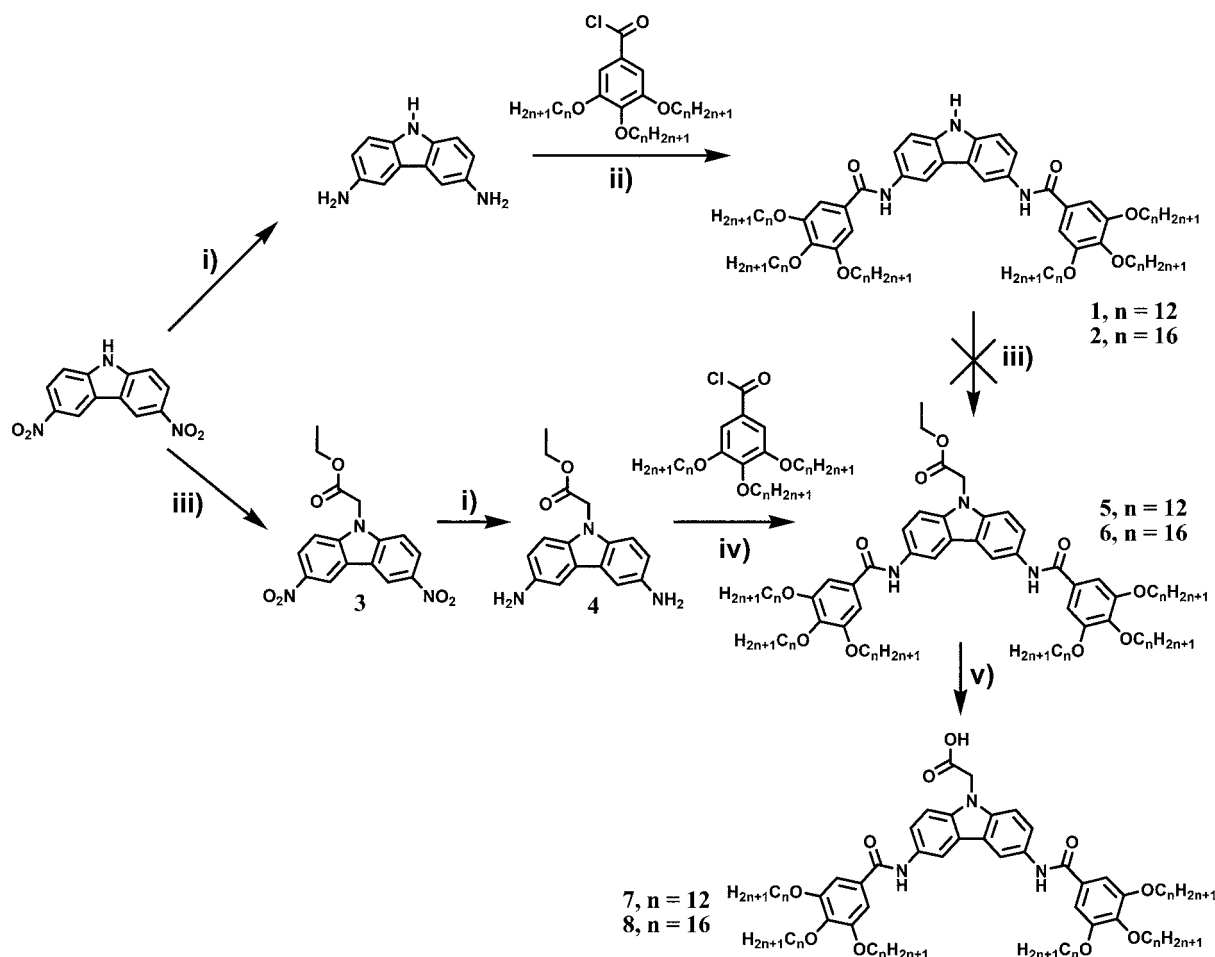
3,6-Dinitrocarbazole and 3,6-diaminocarbazole were synthesized according to reported procedures.<sup>23</sup> Scheme 1 outlines the

synthetic procedures for compounds **1–8** containing carbazole cores. Compounds **1** with  $n = 12$  and **2** with  $n = 16$  were readily obtained by reaction of the 3,6-diaminocarbazole with 3,4,5-trialkyloxybenzoic acid chloride ( $n = 12, 16$ ) under anhydrous conditions. Unfortunately, reactions of the anions of compounds **1** and **2** with ethylbromoacetate did not allow introduction of the ester function onto the nitrogen atom. Consequently, the ester function was introduced onto the 3,6-dinitrocarbazole starting material. Compound **3** was obtained, in good yield, by addition of a DMF solution of ethylbromoacetate containing the anion of 3,6-dinitrocarbazole preformed by reaction with sodium hydride. Reduction of the nitro fragments on palladium/carbon in methanol with glacial acetic acid afforded compound **4** in 82% yield. The amide-functionalized platforms **5** and **6**, carrying an ester function at the tip, were obtained by amidation with 3,4,5-trialkyloxybenzoic acid chloride ( $n = 12, 16$ ) in dry dichloromethane in the presence of triethylamine. Saponification of the ester function under basic conditions afforded the targeted functional acid platforms **7** ( $n = 12$ ) and **8** ( $n = 16$ ). Purification of the compounds was achieved by chromatography on silica gel followed by crystallization in a  $\text{CH}_2\text{Cl}_2$ – $\text{CH}_3\text{CN}$  mixture. Purity of the samples was probed by  $^1\text{H}$  and  $^{13}\text{C}$  NMR, mass spectroscopy and elemental analysis.

A similar synthetic route was used to build the luminescent naphthalene core, containing an acid function at the tip and two amido-gallate fragments as peripheral structural fragments (Scheme 2). The starting compound 3,6-dinitro-1,8-naphthalic anhydride was synthesized according to literature procedures.<sup>24</sup> Introduction of the ethylacetate fragment was achieved using glycine ethylester hydrochloride under basic conditions affording compound **9** in reasonable yield. Reduction of the nitro functions was efficiently performed under microwave irradiation in the presence of palladium on carbon (10 wt%) and ammonium formate as a solid source of hydrogen.<sup>25</sup> The mixture was heated at 120 °C with stirring for 15 min in a 50 mL reactor vessel under microwave irradiation (300 W). After crystallization, compound **10** was isolated in an almost quantitative yield.

Reaction of compound **10** with 3,4,5-trialkyloxybenzoic acid chloride ( $n = 12, 16$ ) in dry dichloromethane and triethylamine afforded the naphthalene based platforms **11** ( $n = 12$ ) and **12** ( $n = 16$ ) containing an ester function at the tip and two lateral amido-gallate fragments. Finally, the targeted naphthalene platforms **13** ( $n = 12$ ) and **14** ( $n = 16$ ) containing an acid function were obtained by saponification with KOH. Purification of the compounds was achieved by chromatography on silica gel and the purity determined by  $^1\text{H}$  and  $^{13}\text{C}$  NMR, mass spectroscopy and IR spectroscopy. In order to further extend and modify the functionality of the platform, compound **14** was reacted with excess ethylenediamine in the presence of 1-[3-(dimethylamino)propyl]-3-ethylcarbodiimide hydrochloride (EDCI) and dimethylamino pyridine (DMAP) to afford the modified platform **15** carrying a flexible amine function at the central position.

In a final trial the linkage of compounds **8** and **15** was achieved using classical peptide chemistry with EDCI in the presence of DMAP in dry dichloromethane. The flexible dyad **16** containing a naphthalene core and a carbazole residue was produced in 53% isolated yield (Scheme 3).



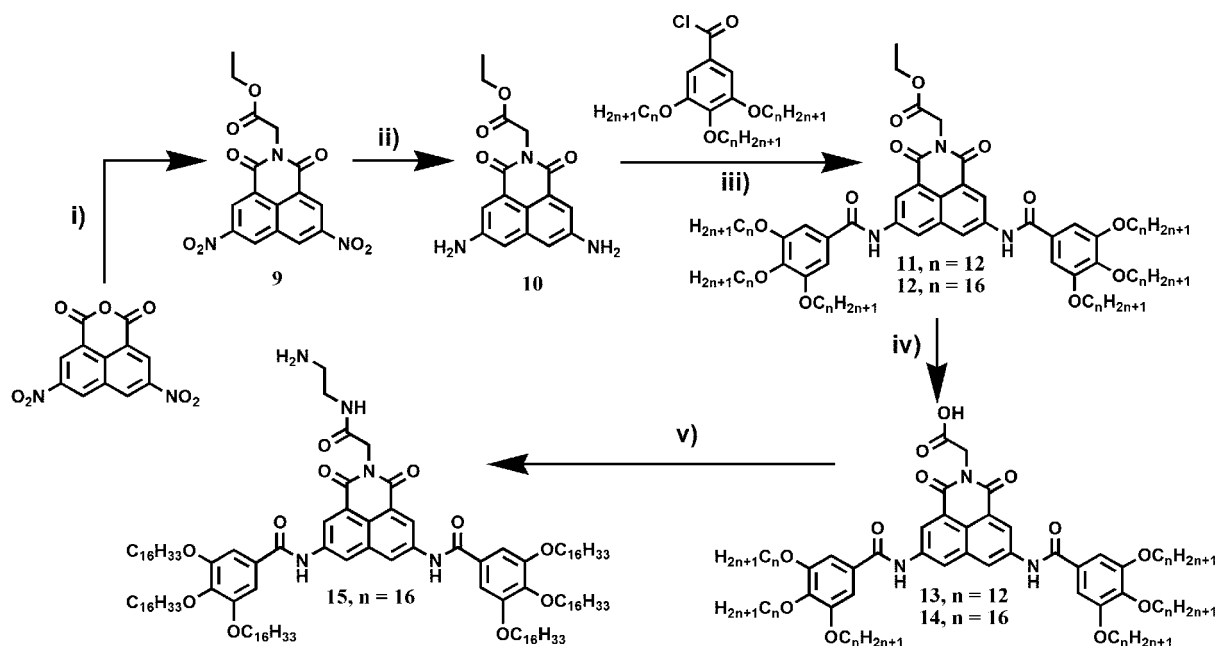
**Scheme 1** Synthesis of the functional carbazole platforms: i) Pd/C (10 w%), glacial acetic acid, MeOH, H<sub>2</sub> (gas, 1 atm), 14 h, rt, 82% for **4** and 80% for 3,6-diaminocarbazole; ii) Et<sub>3</sub>N (4 eq.), THF, rt, 17 h, 48% ( $n = 12$ ), 55% ( $n = 16$ ); iii) NaH (1 eq.), DMF, 30 min, rt, then ethylbromoacetate (1.5 eq.), 20 h, rt, 82%; iv) CH<sub>2</sub>Cl<sub>2</sub>, Et<sub>3</sub>N (4 eq.), rt, 24 h, 47% ( $n = 12$ ), 40% ( $n = 16$ ); v) KOH (5 eq.), THF–H<sub>2</sub>O (90/10 v/v), reflux, 16 h, 54% ( $n = 12$ ), 53% ( $n = 16$ ).

### Spectroscopic properties in solution

Spectroscopic data for compounds **1** to **16** in diluted dichloromethane solutions are gathered in Table 1. All the absorption spectra of the functional carbazole-based platforms **1–2** and **5–8** show a main absorption band with two maxima at 301 nm ( $\epsilon \approx 50\,000\text{ M}^{-1}\text{ cm}^{-1}$ ) and at 261 nm ( $\epsilon \approx 30\,000\text{ M}^{-1}\text{ cm}^{-1}$ ) (Fig. 1a). These absorption bands are assigned to  $\pi$ – $\pi^*$  and  $n$ – $\pi^*$  transitions localized on the carbazole core and the alkoxyphenyl fragments, respectively. The absorption properties are not sensitive to the nature of the substituent on the nitrogen atom. In contrast the spectra of precursors **3** and **4** appear to be quite different and show several absorption bands in the 230–400 nm range (Table 1). Introduction of amino functions on the carbazole core in compound **4** leads to the appearance of a charge transfer band centred at 373 nm. The absorption spectrum of the starting nitro naphthalene derivative **9** displays two main absorption bands at 331 nm ( $\epsilon \approx 7\,000\text{ M}^{-1}\text{ cm}^{-1}$ ) and at 269 nm ( $\epsilon \approx 40\,000\text{ M}^{-1}\text{ cm}^{-1}$ ). Conversion of the nitro functions into amino functions leads to a bathochromic shift of 80 nm of the low energy absorption band and a hypsochromic shift of the high energy absorption band of 20 nm. Absorption spectra of naphthalene platforms **11–15** display two main broad absorption

bands, each displaying two close maxima at 388/376 ( $\epsilon \approx 12\,000\text{ M}^{-1}\text{ cm}^{-1}$ ) and 290/278 nm ( $\epsilon \approx 55\,000\text{ M}^{-1}\text{ cm}^{-1}$ ), respectively (Fig. 1b). The low energy bands are due to transitions mainly localized on the naphthalene core whereas the high energy bands are likely due to  $\pi$ – $\pi^*$  and  $n$ – $\pi^*$  transitions localized on the naphthalene core and the alkoxyphenyl fragments. The nature of the substituent on the diimide fragment did not affect the positions or the absorption coefficients of these bands. The absorption spectrum of dyad **16** displays a broad and intense absorption band presenting a maximum at 299 nm and a weaker absorption peak with a maximum at 380 nm. The absorption spectrum of compound **16** is almost a linear combination of the absorption spectra of compounds **8** and **15** (Fig. 2).

Excitation of the carbazole compounds **1–2** and **5–8** in the lowest energy bands at 301 nm leads to a broad emission band peaking at 400 nm and extending up to 700 nm with low quantum yields (Fig. 1a). In some cases, a second broad emission band centred at 510–520 nm, which appears as a shoulder on the main emission band, can also be detected. In light of previous work,<sup>13,27</sup> this additional broad emissive band is due to aggregates. Whereas the nitro compound **3** is non luminescent, excitation in the lowest energy absorption band of the



**Scheme 2** Synthesis of the functional naphthalene platforms: i) glycine ethylester (1.1 eq.), Et<sub>3</sub>N (1.2 eq.), CH<sub>3</sub>CN, 20 h, 90 °C, 50%; ii) Pd/C (10 w%), EtOH, NH<sub>4</sub>COOH (20 eq.), 300 W, 15 min, 120 °C, 91%; iii) CH<sub>2</sub>Cl<sub>2</sub>, Et<sub>3</sub>N (4 eq.), 20 h, rt, 38% (*n* = 12), 34% (*n* = 16); iv) KOH (5 eq.), THF–H<sub>2</sub>O (90/10 v/v), reflux, 16 h, 88% (*n* = 12), 82% (*n* = 16); v) ethylenediamine (100 eq.), EDCI (2 eq.), DMAP (2 eq.) in dichloromethane at rt, 16 h, 81%.

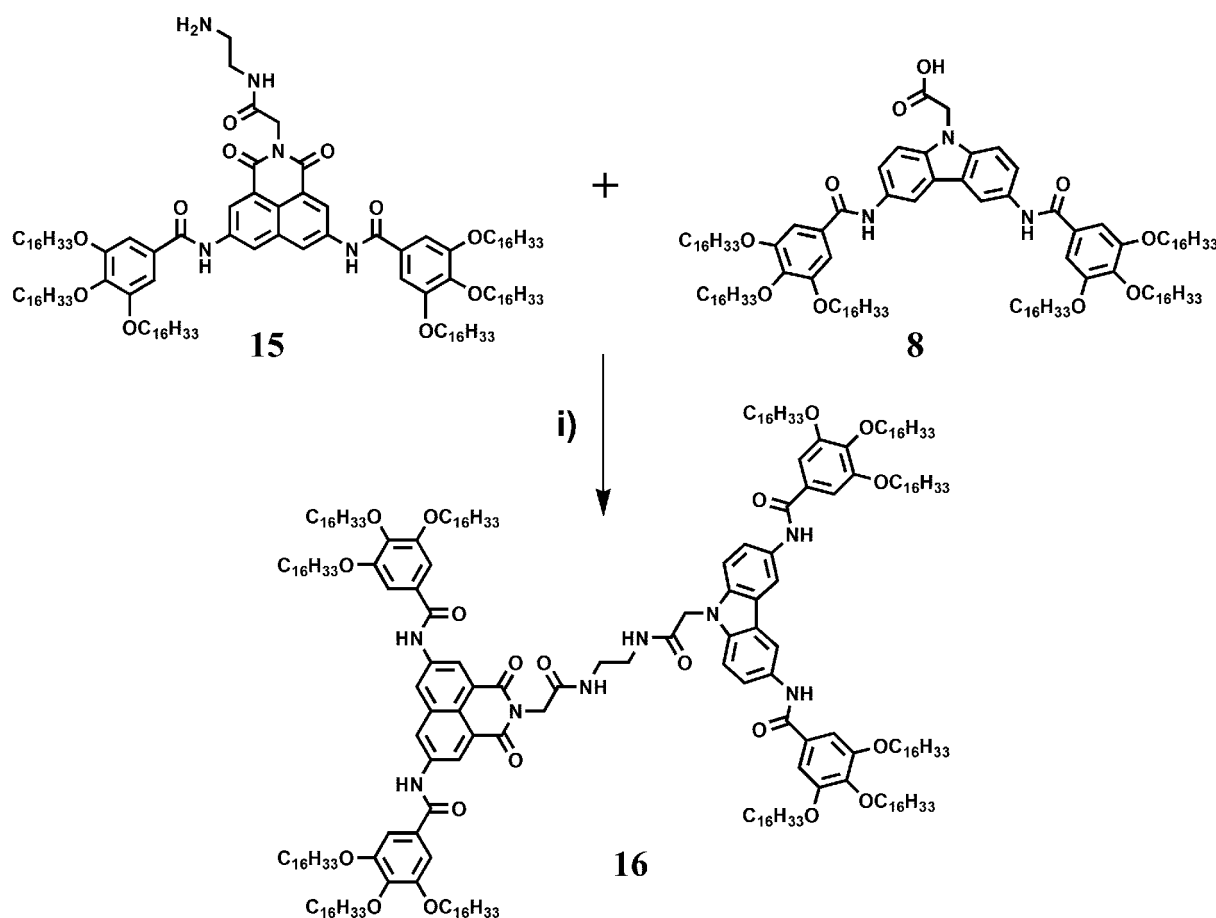
diaminocarbazole derivative **4** at 373 nm leads to a strong emission centred at 424 nm with a quantum yield of 0.25. As for compound **3**, the naphthalene-dinitro compound **9** is not luminescent. This is not very surprising because it has been previously reported that a nitro function is easily reduced, and that when coupled to a chromophore (*e.g.*: cyanines, Bodipy, pyrene and naphthalene...) a photo-induced electron transfer from the excited dye to the nitro residues occurs.<sup>28</sup> Excitation of compound **10** at 412 nm leads to a broad emission centred at 483 nm with a quantum yield of 0.36. As observed above for the amino derivatives **4** and **10**, the electron donating ability of the amino functions improves the luminescent properties of the aromatic core. It was found that compounds **11–16** have a strong tendency to form aggregated species in solution at concentrations above 10<sup>-5</sup> M and, upon excitation at 380 nm, broad emission bands with multiple contributions and that extended from 400 up to 700 nm, were observed. At lower concentrations, the aggregation feature of these dyes is clearly highlighted by excitation at 380 nm leading to a dual emission band centred at 430 nm with an additional broad emission band tailing-off up to 700 nm (Fig. 1b). This is a clear signature of the high tendency of these dyes to aggregate, as would be expected by the design and the presence of a flat core, and amide vectors which likely promote intermolecular hydrogen bonding. The quantum yields determined for this series of compounds lie in the range 0.9–1.3%.

### Thermal studies

The liquid crystalline properties of compounds **1–2**, **5–8**, **11–14**, **15** and **16**, carrying amido-gallate fragments with long alkoxy chains, were investigated by polarizing optical microscopy (POM), differential scanning calorimetry (DSC) and small-angle

X-ray diffraction (SA-XRD). The measured transition temperatures and enthalpy values are gathered in Table 2, whilst the mesophase parameters are gathered in Table 3.

**Thermal behaviour of the carbazole derivatives 1–8.** Both carbazole compounds **1** and **2** (with chain-length *n* = 12 and *n* = 16, respectively) behave quite similarly and display two reversible thermal transitions, as detected by DSC (Table 2). POM observations revealed that the high transition temperature, at about 100 °C for both samples, corresponds to the cooling temperature. Upon cooling, DSC traces evidenced a slight supercooling of the transition, at about 80 °C, as observed by POM. The materials are still fluid at this temperature and birefringence can be induced by mechanical stress, suggesting the formation of a liquid crystalline mesophase. On further cooling, a broad transition is detected by DSC which is likely attributed to crystallization of aliphatic chains, through the hardening of the material. X-Ray patterns recorded in the temperature range from 20 to 120 °C confirmed the above observations and allowed the identification of the mesophases for both compounds. In the temperature intervals delimited by DSC and POM, and which correspond to mesophase stability, one intense and several weak, sharp, small-angle diffraction peaks along with broad wide-angle diffuse bands were detected. For compound **1** (Fig. 3), reflections, with spacings in the ratio 1:√3:√4:√9:√13 could be indexed unequivocally as the *hk* reflections (10), (11), (20), (30), (31) of a hexagonal lattice with *p6mm* plane symmetry. In the wide angle part, the very intense halo centred at 4.6 Å was associated with the molten chains in the isotropic state, and the two weak diffusions at 3.8 and 7.5 Å, to some intermolecular interactions (*vide supra*). For **2**, the same wide-angle features were observed (*h*, *h'*, *h<sub>ch</sub>*), but only two sharp small-angle peaks were detected, indexed by analogy to **1** as (10) and (30) reflections of the hexagonal



**Scheme 3** Chemical structure of the functional dyad. Key: i) EDCI (2 eq.), DMAP (2 eq.) in dichloromethane at rt, 16 h, 53%.

lattice. Although, the phases assignment as  $\text{Col}_h$  is not unequivocal (the small-angle reflections are indeed compatible with a smectic phase too), it is nevertheless more reasonable to consider the columnar morphology because of the semi-disc-like shape of the compound and to the recognized columnar mesophase nature of its lower-chain counterpart. Such an assumption is also strongly supported and consistent with the behaviour reported for other structurally related bent hexacatenar liquid crystals.<sup>29</sup> Thus, both compounds exhibit a  $\text{Col}_h$  phase, with lattice parameters at 80 °C of 44.4 and 49.2 Å for **1** and **2**, respectively, which are quasi invariant with temperature (Table 3).

The corresponding ester carbazole derivatives **5** ( $n = 12$ ) and **6** ( $n = 16$ ), exhibit a completely different thermal behaviour. The DSC traces of **5** display an endothermic peak centred at 112 °C, and a broad exothermic peak centred at 82 °C on the heating and cooling curves, respectively. By POM, **5** is in the isotropic state at 112 °C, and below 82 °C on cooling, turns slightly birefringent but no readily developed texture occurs. DSC traces of compound **6** reveal the presence of a single broad reversible thermal transition centred at 86 °C on heating, associated to the isotropization (POM). Both compounds exhibit strong supercooling. XRD demonstrated in both cases the absence of a liquid crystalline phase, despite the birefringence exhibited by both samples. Instead, only broad and intense reflections, seen at *ca* 27 and 4.5 Å for **5** and *ca* 35 and

4.5 Å for **6**, were detected, which suggested amorphous solids with partial ordering.

The initial DSC heating curves of compounds **7** and **8**, the acid parents of **5** and **6**, respectively, displayed broad transitions, due to some internal rearrangement and melting of the aliphatic chains. After thermal treatment, compound **7** displays a single broad reversible transition centred at 23 °C, corresponding to melting. As for **8**, after the first heating curve, the compound did not show any thermal transition from –20 °C up to 110 °C; POM observations revealed its non-mesomorphic nature in the explored temperature range. Thus, among the six carbazole derivatives, only the non-substituted carbazoles, **1** and **2**, are mesomorphic, exhibiting a  $\text{Col}_h$  mesophase, showing that small modifications of the core's tip is detrimental to the emergence of liquid crystallinity.

**Thermal behaviour of the naphthalene derivatives 11–16.** In contrast to the thermal behaviour of the carbazole-based compounds, most of the compounds derived from the naphthalene core were mesomorphic. At room temperature, compound **11** (with dodecyl chains) with a naphthalene core carrying an ester function appears as a birefringent sticky material. DSC traces displayed two reversible thermal transitions centred at 161 °C and 221 °C (Fig. 4a), the higher one corresponding to the transition to the isotropic liquid (above 221 °C, the compound is an isotropic fluid).

**Table 1** Optical data measured in dichloromethane solution at 298 K

| Compd | $\lambda_{\text{abs}}/\text{nm}$ ( $\epsilon/\text{M}^{-1} \text{cm}^{-1}$ ) | $\lambda_{\text{F}}/\text{nm}$ @ $\lambda_{\text{ex}}/\text{nm}$ | $\Phi_{\text{F}}^a$ |
|-------|--|--|---------------------|
| 1     | 301 (51 600)   | 416 @ 301  | <0.01               |
|       | 259 (32 750)   | 513 @ 301  |                     |
| 2     | 301 (48 600)   | 395 @ 301  | <0.01               |
|       | 259 (29 800)   | 513 @ 301  |                     |
| 3     | 358 (16 900)   | —  | —                   |
|       | 267 (27 200)   | —  |                     |
|       | 286 (18 800)   | —  |                     |
| 4     | 373 (3 100)  | 424 @ 373  | 0.25                |
|       | 319 (9 100)  | —  |                     |
|       | 235 (24 250)   | —  |                     |
| 5     | 301 (45 700)   | 399 @ 301  | <0.01               |
|       | 261 (30 100)   | —  |                     |
| 6     | 301 (50 700)   | 417 @ 301  | <0.01               |
|       | 261 (33 100)   | 517 @ 301  |                     |
| 7     | 301 (49 200)   | 398 @ 301  | <0.01               |
|       | 260 (32 000)   | —  |                     |
| 8     | 300 (47 700)   | 398 @ 301  | <0.01               |
|       | 261 (34 100)   | 520 @ 301  |                     |
| 9     | 331 (7 400)  | —  | —                   |
|       | 269 (40 700)   | —  |                     |
|       | 412 (8 000)  | 483 @ 390  |                     |
| 10    | 250 (37 800)   | 483 @ 390  | 0.36                |
|       | 388 (12 600)   | 429 @ 390  |                     |
| 11    | 376 (12 800)   | —  | 0.013               |
|       | 291 (60 000)   | —  |                     |
|       | 278 (59 400)   | —  |                     |
|       | 388 (10 800)   | 431 @ 380  |                     |
|       | 376 (11 200)   | —  |                     |
| 12    | 290 (54 400)   | —  | 0.012               |
|       | 277 (54 300)   | —  |                     |
|       | 388 (13 200)   | 428 @ 380  |                     |
|       | 377 (13 500)   | —  |                     |
|       | 290 (60 600)   | —  |                     |
| 13    | 278 (60 800)   | —  | 0.013               |
|       | 388 (13 400)   | 429 @ 380  |                     |
|       | 378 (13 600)   | —  |                     |
|       | 290 (53 500)   | —  |                     |
|       | 278 (53 350)   | —  |                     |
| 14    | 388 (11 700)   | 430 @ 380  | 0.011               |
|       | 376 (12 100)   | —  |                     |
|       | 289 (53 100)   | —  |                     |
|       | 279 (52 700)   | —  |                     |
|       | 298 (100 500)  | —  |                     |
| 15    | 388 (7 700)  | 429 @ 380  | 0.009               |
|       | 298 (100 500)  | —  |                     |
|       | 298 (100 500)  | —  |                     |

<sup>a</sup> Determined in dichloromethane solution ( $c \approx 10^{-7}$  M) using Rhodamine 6G as reference ( $\Phi_{\text{F}} = 0.78$  in water,  $\lambda_{\text{exc}} = 488$  nm).<sup>26</sup> All  $\Phi_{\text{F}}$  are corrected for changes in refractive index.

On cooling of the isotropic liquid, the compound becomes birefringent and broken-fan shaped textures and large homeotropic domains, typical of a hexagonal columnar phase, were observed (Fig. 5a). The fluid nature of the material confirms its liquid-crystalline nature. Below the low-temperature transition (145 °C), the homeotropic domains become birefringent and the birefringence properties and the size of the fan-shaped domains are concomitantly strongly affected (Fig. 5b).

Such changes in the birefringence and textural properties are usually attributed to a high-to-low symmetry phase transformation (e.g. a hexagonal/rectangular lattice phase transformation). The homologous derivative with hexadecyl chains, **12**, has a thermal behaviour close to **11**, with two reversible thermal transitions visible by DSC. Above 192 °C, the material is an isotropic liquid. Cooling below 189 °C leads to the formation of a mosaic-like texture with pseudo-fan shapes typical of

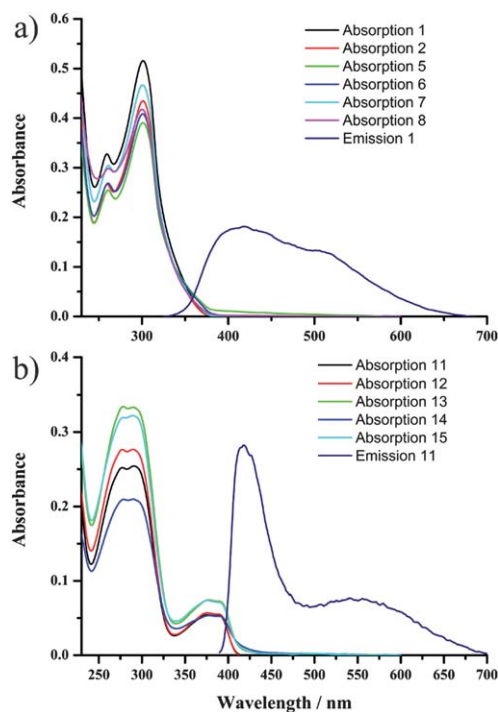


**Fig. 1** a) Absorption spectra of compounds **1–2** and **5–8** in dichloromethane and an emission spectrum of compound **1** ( $\lambda_{\text{ex}} = 301$  nm) in dichloromethane ( $c \approx 1.0 \times 10^{-6}$  mol L<sup>-1</sup>) as a typical example (arbitrary unit); b) absorption spectra of compounds **11–15** in dichloromethane and an emission spectrum of compound **11** ( $\lambda_{\text{ex}} = 380$  nm) in dichloromethane ( $c \approx 1.0 \times 10^{-6}$  mol L<sup>-1</sup>) as a typical example (arbitrary unit).

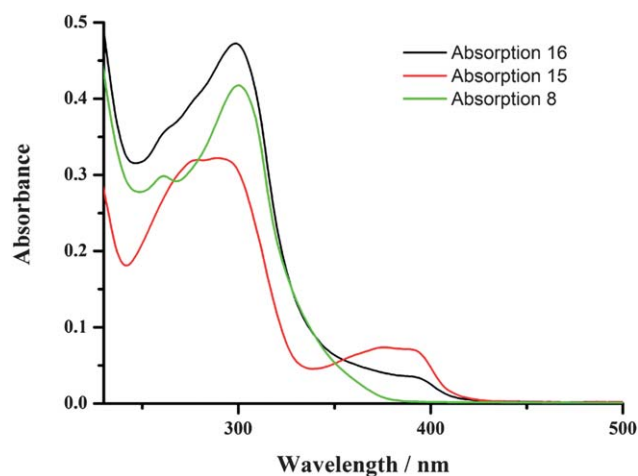


**Fig. 2** Absorption spectra of compounds **8**, **15** and dyad **16** in dichloromethane.

a hexagonal columnar mesophase, and below 141 °C the textural changes indicate the formation of another columnar mesophase, likely with a rectangular symmetry, as above. On further cooling, two other additional reversible thermal transitions centred at 33 and 25 °C were detected by DSC. Based on POM, these transitions are likely attributed to mesophase/crystal and crystal/crystal phase transitions, respectively. XRD confirmed the existence of two mesophases for each compounds, namely a

**Table 2** Thermal behaviour of compounds **1–2**, **5–8**, **11–14**, **15** and **16**.<sup>a</sup>

| Compd     | Onset transition temperatures/°C ( $\Delta H = \text{enthalpy/kJ mol}^{-1}$ )                                  |   |
|-----------|--|---|
|           | 2nd Heating  | 1st Cooling   |
| <b>1</b>  | Cr 29 (13.8) Col <sub>h</sub> 100 (26.15) Iso  | Iso 82 (–21.5) Col <sub>h</sub> 22(–13.75) Cr   |
| <b>2</b>  | Cr 57.5 (42.3) Col <sub>h</sub> 98 (21.8) Iso  | Iso 81 (–21.4) Col <sub>h</sub> 52 (–31.05) Cr  |
| <b>5</b>  | M 112 (13.7) Iso   | Iso 82 (–6.9) M   |
| <b>6</b>  | M 86 (66.9) Iso  | Iso 16 (–63.4) M  |
| <b>7</b>  | Cr 23 (56.2) Iso   | Iso 20 (–55.6) Cr   |
| <b>8</b>  | –20 Iso 110  | 110 Iso –20   |
| <b>11</b> | Col <sub>r</sub> 161 (19.4) Col <sub>h</sub> 221 (7.5) Iso   | Iso 219 (–7.5) Col <sub>h</sub> 145 (–16.9) Col <sub>r</sub>  |
| <b>12</b> | Cr 28 (18.5) Cr' 42 (27.7) Col <sub>o</sub> 120 (–) Col <sub>r</sub> 150 (15.5) Col <sub>h</sub> 192 (7.5) Iso | Iso 189 (–6.9) Col <sub>h</sub> 141 (–14.1) Col <sub>r</sub> 50 (–) Col <sub>o</sub> 33 (–27.9) Cr' 25 (–18.3) Cr |
| <b>13</b> | Col <sub>h</sub> 235 (4.3) Iso   | Iso 228 (–4.2) Col <sub>h</sub>   |
| <b>14</b> | Cr 28 (89.8) Col <sub>h</sub> 209 (6.8) Iso  | Iso 204 (–5.6) Col <sub>h</sub> 22 (–91.2) Cr   |
| <b>15</b> | Cr 21 (71.4) Col <sub>h</sub> 230 (30.1) iso   | Iso (24.3) 230 Col <sub>h</sub> 19 (–71.8) Cr   |
| <b>16</b> | Cr 31 (179.8) Col <sub>h</sub> 110 (–) Iso   | Iso (–) 105 Col <sub>h</sub> 24 (–175.1) Cr   |

<sup>a</sup> Cr, crystalline phase; Iso, isotropic liquid; Col<sub>h</sub>, hexagonal columnar mesophase; Col<sub>r</sub>, rectangular columnar mesophase; Col<sub>o</sub>, oblique columnar phase; M, amorphous solid.

high-temperature Col<sub>h</sub> phase and a Col<sub>r</sub> at lower temperature. The Col<sub>h</sub> phase of both compounds was identified by the presence of three small-angles, sharp reflections, indexed as  $hk$  reflections (10), (11), (20) of a hexagonal lattice with the  $p6mm$  plane symmetry. In the wide angle part, the very intense halo centred at 4.6 Å was associated with the molten chains in the isotropic state, and another weak diffusion at 3.5–3.8 Å, associated to the short-range stacking of the naphthalene cores (vide supra). The lower-temperature mesophase X-ray pattern exhibited broad diffusions, as above for the Col<sub>h</sub> phases, evidencing the molten state of the alkyl chains and the persistence, although short-range, of the stacking, and a series of sharp, small-angle peaks. Despite the presence of only one single intense and sharp peak (fundamental reflection), the X-ray pattern was not compatible with hexagonal and square lattices, and therefore were excluded. However, considering this single peak as the 11/20 reflection, indexation of all peaks was in agreement with a rectangular lattice with the  $p2gg$  plane group (Table 3); this particular rectangular phase, with lattice ratio  $a/b = \sqrt{3}$  is also known as pseudo-hexagonal phase.<sup>30</sup> In addition, **12** exhibits another mesophase at a lower temperature than the Col<sub>r</sub> phase that could be detected by XRD only, through the shift of some of the small-angle reflections and the emergence of new ones. The absence of any apparent changes on the DSC heating trace suggests a second order phase transition, occurring at *ca* 120 °C, but that supercools strongly (transition below 60 °C). On the basis of the X-ray patterns obtained from this mesophase, the small-angle reflections could be indexed into an oblique lattice with the  $p-1$  plane symmetry, *i.e.* the mesophase is an oblique columnar phase, Col<sub>o</sub>; the fluid nature of the phase was also confirmed by the presence of broad diffuse bands in the wide-angle area.

The pendant naphthalene acid derivatives (**13** and **14**) appear also to be mesomorphic too. DSC traces of **13** displayed a single reversible transition centred at 235 °C, above which the material is isotropic. Upon cooling, a fluid birefringent phase forms and a pseudo-fan shaped texture typical of columnar hexagonal phase readily develops (POM). Lengthening of the chains (**14**) allows its crystallization at low temperature and an energetic

reversible broad transition, attributed to the crystallization of the aliphatic chains, is detected on the DSC traces around 28 °C (on the heating curve, Fig. 4b). At 209 °C, a low enthalpy transition is detected and POM observations reveal that this transition is associated with the isotropization temperature. A thin mosaic-like texture is observed by POM in the 50–200 °C temperature range. The hexagonal symmetry of the columnar mesophase was readily confirmed by XRD where two and three sharp reflections, (10), (11), (20), were detected in the small angle and three diffuse scatterings in the wide part,  $h'$ ,  $h_{ch}$  and  $h$ . As above, for compounds **1** and **2**, respectively, these halos correspond to the molten state of the alkyl chains ( $h_{ch}$ ) and to some intermolecular interactions ( $h$ ,  $h'$ , short-range uniaxial stacking periodicity). In both case, the mesophase lattice parameters are quasi invariant in the mesomorphic temperature ranges (Table 3).

Finally, **15** displays two reversible transitions, at 21 °C, associated with the melting of the hydrocarbon chains, and at 230 °C, the temperature at which the compound clears into the isotropic liquid. POM observations revealed that above 21 °C the material is in a liquid-crystalline state, and mosaic-like textures typical of hexagonal columnar mesophases are observed. Introduction of the ethyl-amine arm thus slightly stabilizes the Col<sub>h</sub> phase with respect to that of **14**, since isotropization occurs at 230 °C. XRD confirmed the presence of a single mesophase between these two temperatures, although only one peak could be detected in the small-angles region, insufficient for a proper mesophase assignment. Supported by POM and by the behaviour of its homologues (**12** and **14**), the phase is likely columnar and was assigned as Col<sub>h</sub>, with a lattice parameter of 44.3 Å.

**Thermal behaviour of the carbazole-naphthalene dyad 16.** Finally, the dyad **16** resulting from the connection of **8** and **15** displays a single broad and reversible thermal transition on the DSC traces at 31 °C. As already mentioned, this broad transition is associated to the melting of the carbon chains. Above this transition, no texture could be observed by POM. Although, mechanical constraints on the top glass cover slide induced the emergence of birefringence. This behaviour can be explained by the strong tendency of the material to form homeotropic

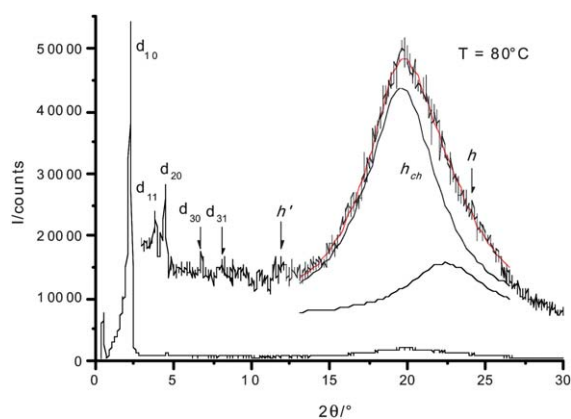
**Table 3** X-Ray diffraction data and mesophase parameters

| $T/^\circ\text{C}^a$ | $d_{\text{exp}}/\text{\AA}^b$ | I/L     | $hk^c$          | $d_{\text{theo}}/\text{\AA}^{bd}$    | Parameters <sup>ef</sup>  |
|----------------------|-------------------------------|---------|-----------------|--------------------------------------|---|
| <b>1</b>             | 38.4                          | VS (sh) | 10              | 38.45                                | $T = 80^\circ\text{C}$  |
|                      | 22.23                         | M (sh)  | 11              | 22.20                                | $\text{Col}_h\text{-}p6mm$  |
|                      | 19.17                         | M (sh)  | 20              | 19.22                                | $a = 44.4 \text{\AA}$   |
|                      | 12.75                         | M (sh)  | 30              | 12.82                                | $S = 1710 \text{\AA}^2$   |
|                      | 10.74                         | M (sh)  | 31              | 10.66                                | $V_{\text{mol}} = 2610 \text{\AA}^3$  |
|                      | 7.5                           | W (br)  |                 | $h'$                                 | $h_0 = 3.05 \text{\AA}$ for $Z = 2$   |
|                      | 4.6                           | VS (br) |                 | $h_{\text{ch}}$                      |   |
| <b>2</b>             | 3.8                           | W (br)  |                 | $h$                                  |   |
|                      | 42.75                         | VS (sh) | 10              | 42.6                                 | $T = 80^\circ\text{C}$  |
|                      | 14.15                         | M (sh)  | 30              | 14.2                                 | $\text{Col}_h\text{-}p6mm$  |
|                      | 7.4                           | W (br)  |                 | $h'$                                 | $a = 49.2 \text{\AA}$   |
|                      | 4.6                           | VS (br) |                 | $h_{\text{ch}}$                      | $S = 2095 \text{\AA}^2$   |
| <b>11</b>            | 3.6                           | W (br)  |                 | $h$                                  | $V_{\text{mol}} = 3195 \text{\AA}^3$  |
|                      | 29.22                         | VS (sh) | 11/20           | —                                    | $T = 120^\circ\text{C}$   |
|                      | 22.5                          | VS (sh) | 21              | 22.1                                 | $\text{Col}_r\text{-}p2gg$  |
|                      | 16.0                          | W (sh)  | 12              | 16.2                                 | $a = 58.4 \text{\AA}$   |
|                      | 13.2                          | M (sh)  | 41              | 13.4                                 | $b = 33.72 \text{\AA}$  |
|                      | 4.7                           | VS (br) |                 | $h_{\text{ch}}$                      | $S = 984.5 \text{\AA}^2$  |
|                      | 3.7                           | W (br)  |                 | $h$                                  | $V_{\text{mol}} = 3000 \text{\AA}^3$  |
|                      |                               |         |                 |                                      | $h_0 = 3.05 \text{\AA}$ for $Z = 1$   |
|                      | 28.9                          | VS (sh) | 10              | 28.87                                | $T = 180^\circ\text{C}$   |
|                      | 16.62                         | S (sh)  | 11              | 16.67                                | $\text{Col}_h\text{-}p6mm$  |
|                      | 14.47                         | M (sh)  | 20              | 14.43                                | $a = 33.3 \text{\AA}$   |
| 4.6                  | VS (br)                       |         | $h_{\text{ch}}$ | $S = 965 \text{\AA}^2$               |   |
| 3.5                  | M (br)                        |         | $h$             | $V_{\text{mol}} = 3015 \text{\AA}^3$ |   |
| <b>12</b>            |                               |         |                 |                                      | $h_0 = 3.1 \text{\AA}$ for $Z = 1$  |
|                      | 33.44                         | VS (sh) | 11              | —                                    | $T = 80^\circ\text{C}$  |
|                      | 30.75                         | VS (sh) | 1-1             | —                                    | $\text{Col}_o\text{-}p\text{-}1$  |
|                      | 26.22                         | S (sh)  | 20              | —                                    | $a = 52.64 \text{\AA}$  |
|                      | 21.73                         | S (sh)  | 2-1             | 21.2                                 | $b = 40.6 \text{\AA}$   |
|                      | 18.29                         | VS (sh) | 1-2             | 18.33                                | $\gamma = 85^\circ$   |
|                      | 16.84                         | W (sh)  | 31/22           | 16.6/16.7                            | $S = 1060 \text{\AA}^2$   |
|                      | 14.17                         | W (sh)  | 32              | 13.8                                 | $V_{\text{mol}} = 3500 \text{\AA}^3$  |
|                      | 12.75                         | W (sh)  | 41/1-3          | 12.8                                 | $h_0 = 3.3 \text{\AA}$ for $Z = 1$  |
|                      | 4.75                          | VS (br) |                 | $h_{\text{ch}}$                      |   |
|                      | 3.8                           | M (br)  |                 | $h$                                  |   |
|                      | 32.8                          | VS (sh) | 11/20           | —                                    | $T = 140^\circ\text{C}$   |
|                      | 24.32                         | VS (sh) | 21              | 24.8                                 | $\text{Col}_r\text{-}p2gg$  |
|                      | 18.8                          | S (sh)  | 31/02           | 18.94                                | $a = 65.6 \text{\AA}$ , $b = 37.87 \text{\AA}$  |
|                      | 17.85                         | S (sh)  | 12              | 18.2                                 | $S = 1242 \text{\AA}^2$   |
|                      | 14.7                          | M (sh)  | 32/41           | 14.3/15.05                           | $V_{\text{mol}} = 3500 \text{\AA}^3$  |
|                      | 4.7                           | VS (br) |                 | $h_{\text{ch}}$                      | $h_0 = 3.05 \text{\AA}$ for $Z = 1$   |
| 3.7                  | M (br)                        |         | $h$             |                                      |   |
| <b>13</b>            | 32.3                          | VS (sh) | 10              | 32.24                                | $T = 160^\circ\text{C}$   |
|                      | 18.6                          | S (sh)  | 11              | 18.61                                | $\text{Col}_h\text{-}p6mm$  |
|                      | 16.1                          | S (sh)  | 20              | 16.12                                | $a = 37.23 \text{\AA}$  |
|                      | 7.8                           | M (br)  |                 | $h'$                                 | $S = 1200 \text{\AA}^2$   |
|                      | 4.6                           | VS (br) |                 | $h_{\text{ch}}$                      | $V_{\text{mol}} = 3590 \text{\AA}^3$  |
|                      | 3.8                           | M (sh)  |                 | $h$                                  | $h_0 = 3.0 \text{\AA}$ for $Z = 1$  |
|                      | 26.86                         | VS (sh) | 10              | 26.84                                | $T = 160^\circ\text{C}$   |
|                      | 15.48                         | M (sh)  | 11              | 15.49                                | $\text{Col}_h\text{-}p6mm$  |
|                      | 8.0                           | M (br)  |                 | $h'$                                 | $a = 30.99 \text{\AA}$  |
|                      | 4.7                           | VS (br) |                 | $h_{\text{ch}}$                      | $S = 830 \text{\AA}^2$  |
| <b>14</b>            | 3.75                          | M (br)  |                 | $h$                                  | $V_{\text{mol}} = 2925 \text{\AA}^3$  |
|                      |                               |         |                 |                                      | $h_0 = 3.5 \text{\AA}$ for $Z = 1$  |
|                      |                               |         |                 |                                      | $a = 30.63, 30.8, 31.41, \text{ and } 31.98 \text{ at } T = 120, 140, 180 \text{ and } 200^\circ\text{C}$ |
|                      | 30.05                         | VS (sh) | 10              | 29.9                                 | $T = 140^\circ\text{C}$   |
|                      | 17.31                         | S (sh)  | 11              | 17.26                                | $\text{Col}_h\text{-}p6mm$  |
|                      | 14.84                         | M (sh)  | 20              | 14.95                                | $a = 34.52 \text{\AA}$  |
|                      | 8.0                           | M (br)  |                 | $h'$                                 | $S = 1030 \text{\AA}^2$   |
| 4.7                  | VS (br)                       |         | $h_{\text{ch}}$ | $V_{\text{mol}} = 3490 \text{\AA}^3$ |   |
| 3.8                  | M (br)                        |         | $h$             | $h_0 = 3.45 \text{\AA}$ for $Z = 1$  |   |
| <b>15</b>            |                               |         |                 |                                      | $a = 34.4, 34.6, 34.7, 34.9, 35.1 \text{ at } T = 120, 140, 160, 180 \text{ and } 200^\circ\text{C}$      |
|                      | 38.4                          | VS (sh) | 10              | 38.4                                 | $T = 100^\circ\text{C}$   |
|                      | 4.7                           | VS (br) |                 | $h_{\text{ch}}$                      | $\text{Col}_h\text{-}p6mm$  |
|                      |                               |         |                 |                                      | $a = 44.3 \text{\AA}$   |
|                      |                               |         |                 |                                      | $S = 1700 \text{\AA}^2$   |
|                      |                               |         |                 | $V_{\text{mol}} = 3490 \text{\AA}^3$ |   |
|                      |                               |         |                 | $h_0 = 4.7 \text{\AA}$ for $Z = 2$   |   |

Table 3 (Contd.)

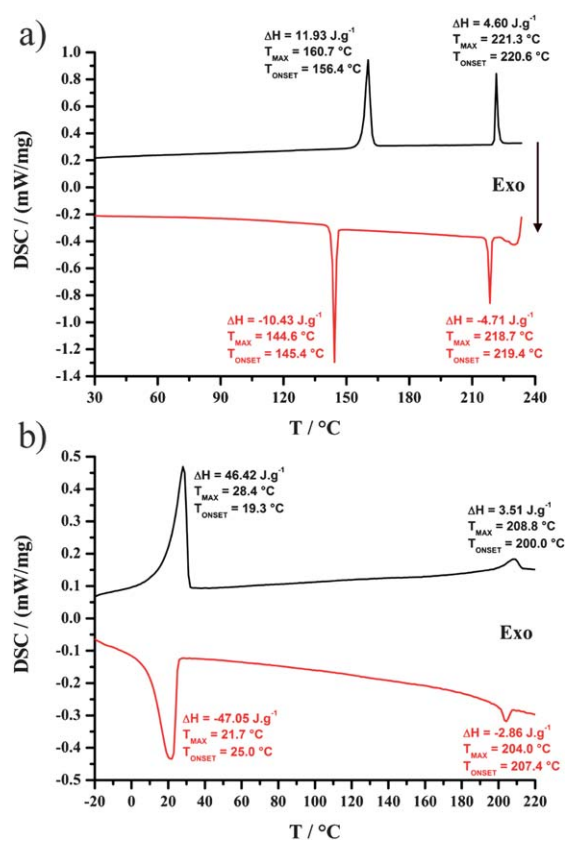
| $T/^\circ\text{C}^a$ | $d_{\text{exp}}/\text{\AA}^b$ | I/L     | $hk^c$          | $d_{\text{theo}}/\text{\AA}^{bd}$ | Parameters <sup>ef</sup>             |
|----------------------|-------------------------------|---------|-----------------|-----------------------------------|--------------------------------------|
| 16                   | 33.16                         | VS (sh) | 10              | 33.1                              | $T = 100^\circ\text{C}$              |
|                      | 19.1                          | M (sh)  | 11              | 19.1                              | $\text{Col}_h\text{-}p6mm$           |
|                      | 9.0                           | M (br)  | $h'$            | $h'$                              | $a = 38.2 \text{\AA}$                |
|                      | 4.7                           | VS (br) | $h_{\text{ch}}$ | $h_{\text{ch}}$                   | $S = 1265 \text{\AA}^2$              |
|                      |                               |         |                 |                                   | $V_{\text{mol}} = 6420 \text{\AA}^3$ |
|                      |                               |         |                 |                                   | $h_0 = 4.7 \text{\AA}$ for $Z = 1$   |

<sup>a</sup>  $T$  and  $T^0$  in  $^\circ\text{C}$ ,  $T^0 = 25^\circ\text{C}$ , and  $T$  is the experimental temperature. <sup>b</sup>  $d_{\text{exp}}$  and  $d_{\text{theo}}$  are the experimentally measured and theoretical diffraction spacings. The distances are given in  $\text{\AA}$ . <sup>c</sup>  $[hk]$  are the indexation of the reflections. Intensity of the reflections: VS: very strong, S: strong, M: medium, W: weak, VW: very weak; br and sh stand for broad and sharp (diffuse) reflections, respectively. <sup>d</sup>  $d_{\text{theo}}$  is deduced from the lattice parameter  $a$  ( $\text{Col}_h$ ) from the following mathematical expressions:  $a = 2[\sum_{hk} d_{hk} \cdot (h^2 + k^2 + hk)^{1/2}] / \sqrt{3} \times N_{hk}$  where  $N_{hk}$  is the number of  $hk$  reflections and  $S$  is the lattice area:  $S = a^2 \sqrt{3} / 2$ . For the  $\text{Col}_r$  phase,  $d_{hk} = 1/\sqrt{(h^2/a^2 + k^2/b^2)}$  and  $S = ab/2$ . For the  $\text{Col}_o$  phase,  $a = 2d_{20}/\sin\gamma$  and  $b = A/\sin\gamma$ , where  $A = (2\{(1/d_{11})^2 + (1/d_{1-1})^2 - (1/2d_{20}^2)\})^{1/2}$  and  $S = absin\gamma/2$ . <sup>e</sup>  $h_0$  is the average intracolumnar repeating distance, deduced directly from the measured molecular volume and the columnar cross-section according to  $h_0 = ZV_{\text{mol}}/S$ , where  $Z$  is the aggregation number or the number of molecular equivalents per stratum of column. Three diffuse scatterings were measured  $h$ ,  $h_{\text{ch}}$ , and  $h'$ , corresponding to the intermolecular stacking, the molten chains in the liquid state, respectively and  $h'$  is likely connected to  $h$  ( $h' = 2h$ ). <sup>f</sup>  $V_{\text{mol}}$  is the molecular volume:  $V_{\text{mol}} = (MW/0.6022) \times (V_{\text{CH}_2}(T)/V_{\text{CH}_2}(T^0))$ , where  $MW$  is the molecular weight and  $V_{\text{CH}_2} = 26.5616 + 0.02023T$

Fig. 3 X-Ray pattern recorded at  $80^\circ\text{C}$  for **1** in the  $\text{Col}_h$  phase.

domains between non treated glass slides. Two sharp small-angle reflections were measured by SA-XRD, allowing the unequivocal identification of the mesophase as  $\text{Col}_h$ , with a lattice parameter of  $38.2 \text{\AA}$  at  $100^\circ\text{C}$ . XRD measurements also revealed that this compound is in the isotropic liquid phase above  $110^\circ\text{C}$ , although thermal transition at this temperature was not detected by DSC, suggesting that the mesophase is highly disordered.

The mesomorphism of all the mesogens described here is characterized by the formation of columnar mesophases, and therefore the molecules are likely to stack on top of each other in order to generate columns with circular cross-sections ( $\text{Col}_h$  phase) or non-circular cross-sections ( $\text{Col}_r$  and  $\text{Col}_o$  mesophases).<sup>30</sup> From the experimental data gathered in Table 3, one can conclude that the supramolecular aggregation into columns is different in carbazole derivatives and naphthalene materials, as evidenced by the great variation of the surface lattices areas. For all organic compounds shown here, a density of  $1 \text{ g cm}^{-3}$  was reasonably considered. For compounds **1** and **2**, the formation of columns necessitates the association of two mesogenic carbazoles to fill the large hexagonal lattice, likely in a head-to-head assembly, and to generate “supramolecular” discotic slices  $h_0$ -thick that stack on top of each other into columns. The

Fig. 4 DSC traces of compounds **11** (a) and **14** (b) (second heating curve (black) and first cooling curve (red)).

presence of the short-range periodicities  $h$  and  $h'$  suggests an alternated  $\pi/2$  stack, with a further slight deviation from the lattice plane (*i.e.* the dimer adopts a propeller conformation) to optimize space filling. For these compounds, 12 diverging aliphatic chains are therefore required to fill the available space between hard columnar core hexagonal networks (formed by the rigid molecular parts). As for the naphthalene derivatives **11–14**,

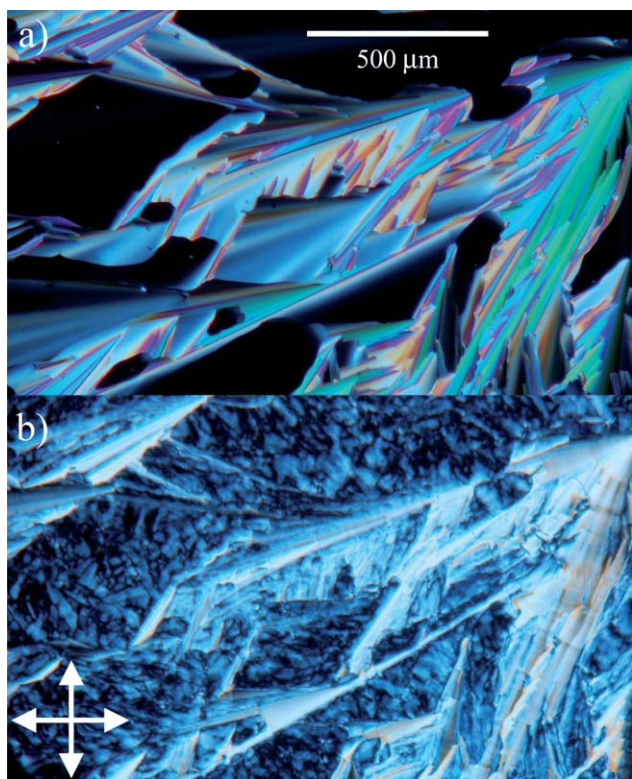


**Fig. 5** Same area of compound **11** observed by optical microscopy at 190 °C (a) and at 130 °C (b) between crossed-polarizers (symbolized by the cross in the corner of the picture).

with small lattices sizes, only one mesogen is necessary to form an elementary columnar slice of thickness  $h_0$  (Table 3), *i.e.* 6 diverging aliphatic chains per slice radiating from the columnar interface, similarly to single discotic molecules. The different symmetries of the planar arrangements of the columns result from a more or less pronounced tilt of the molecular plane with respect to the lattice planes, thus generating a non-circular projection of the columnar cross sections onto the lattice plane, and thus inducing a change in the symmetry.<sup>30</sup> The presence of the two short-range wide-angle periodicities ( $h$  and  $h'$ ) suggests, as above a local alternated  $\pi/2$  stack ordering. The connection of the ethylene diamine fragment yielding **15** results in a change of the self-organisation process as evidenced by a huge increase of the hexagonal lattice (Table 3,  $S$  increases from 1030 Å<sup>2</sup> for **14** to 1700 Å<sup>2</sup> for **15**, *i.e.* about 70% increase, concomitantly with  $h_0$  from 3.45 Å to 4.7 Å). Now, two molecules (12 orthogonal chains per slice) are needed to form the repeat discotic unit, and, as for compounds **1** and **2**, they are likely arranged in a head-to-head manner to be able to pave the hexagonal lattice, although this time the stacking is random, without preferential orientation of the pairs of molecules. Finally, for the 12-chains-containing dyad **16**, only one dimer per  $h_0$  (or two per  $h'$ ) is necessary to generate the columnar organization; the absence of additional signal in the wide-angle part of the diffractogram implies that the molecules are randomly stacked into columns.

FT-IR measurements performed in the mesophases or in the crystalline phases (at 23 °C after heating in the isotropic phase) confirm that the molecular organization is stabilized by hydrogen bonding interactions. All the amide dipoles are involved in

hydrogen bonding, as clearly evidenced by the  $\nu_{\text{NH}}$  and  $\nu_{\text{CO}}$  stretching vibrations that lie respectively in the range 3230–3340 and 1638–1657 cm<sup>-1</sup>. Notice that corresponding values for the free amides are at 3400 cm<sup>-1</sup> for  $\nu_{\text{NH}}$  and around 1680 cm<sup>-1</sup> for  $\nu_{\text{CO}}$ .<sup>13,31</sup> The presence of single  $\nu_{\text{NH}}$ ,  $\nu_{\text{CO}}$  stretching bands in the IR spectra confirms a well-organized hydrogen bonded network in which only one type of hydrogen bond is effective. The frequencies of the bands due to CH<sub>2</sub> antisymmetric and symmetric modes [ $\nu_{\text{a}}(\text{CH}_2)$  and  $\nu_{\text{s}}(\text{CH}_2)$ ] of the alkyl chains appear at *ca* 2914–2921 and *ca* 2850–2852 cm<sup>-1</sup> and indicate that the hydrocarbon chains are all in *trans* conformation.<sup>32</sup> These *trans* peaks at 2920 and 2851 cm<sup>-1</sup> shifted to around 2926 and 2855 cm<sup>-1</sup>, respectively, if the population of the *cis* form in the alkyl chains increases.<sup>33</sup> FTIR measurements performed at room temperature in the liquid crystalline or crystalline phases revealed that the amide functions are involved in hydrogen bonds. These results confirm that the amide function introduced on the platforms play a role in the intermolecular interactions and in the stabilization of the organized phases.

### Solid state luminescence

Temperature-dependent fluorescence measurements were performed in the solid state with a spectrofluorometer equipped with an optical fiber and a heating stage. The carbazole derivatives were found to be non-luminescent in the solid state at room temperature. Emission spectra of the naphthalene derivatives showed a broad emission band centred at 520–540 nm upon excitation at 388 nm at room temperature, whereas a dual emission was observed in fluid solution (Fig. 1b). The red-shift observed on the emission spectra is likely attributed to head-to-tail orientation or J-aggregates of the naphthalene cores in solid state.<sup>34</sup> The evolution of the luminescence of compound **11** in the solid state as a function of the temperature is presented in Fig. 6. Increasing the temperature in the crystalline phase does not significantly change the shape of the emission band but decreases the emission intensity due to non-radiation deactivation pathways. The emission maximum is slightly blue-shifted by about 25 nm upon heating. In the Col<sub>h</sub> phase above 160 °C, the intensity of the luminescence drastically drops and a red-shift of 17 nm is observed. The red-shift observed in the liquid crystalline phase is likely attributed to efficient intermolecular interactions inside the aggregates, favoured by the soft nature of this phase. The fact that the global fluorescence is quenched by increasing the temperature is not surprising and likely due to collisional interactions between ground and excited states which favor non-radiative decay of the fluorescence like in a solid state.<sup>35,36</sup> We thus speculate that in the Col<sub>r</sub> mesophase (below 160 °C) the molecules are less prone to deactivation due to a less favorable structural organization. However, in the Col<sub>h</sub> mesophase (above 160 °C) the molecules are better organized as dimer or oligomers which favor a bathochromic shift of the steady state emission but also a better desactivation in the excited state. Likewise, by cooling the isotropic melt to the various mesophases the spectroscopic behavior is reversible demonstrating the dynamic nature of the fluorophore organization within the mesophases. Upon cooling, the reverse process is observed, excluding decomposition of the materials. At the Col<sub>h</sub>/crystal transition, a blue-shift is observed and the intensity of emitted light

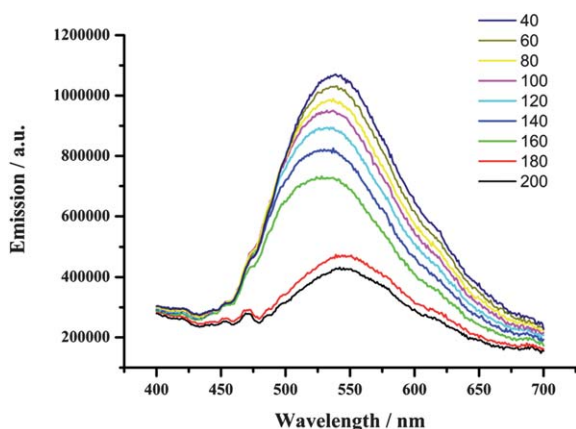


Fig. 6 Solid state emission spectra of compound **11** measured at various temperatures upon heating ( $\lambda_{\text{ex}} = 380$  nm) (2nd heating cycle).

increases, reaching the value of room temperature. The same trend was observed for all the naphthalene platforms.

Recently, it has been demonstrated that luminescence properties of liquid crystalline phases can be exploited to probe the molecular organization in thin films at the macroscopic scale by fluorescence microscopy.<sup>37</sup> For these reasons, the emission properties of compound **11** were evaluated by dependence fluorescence experiments with the help of a fluorescence microscope equipped with a heating stage in the various material states detected by DSC and XRD. Upon cooling from the isotropic state, the materials became liquid-crystalline, enabling formation of homogeneous thin films (Fig. 7a). Well-defined texture can be observed from droplets of the liquid crystalline material by optical microscopy under crossed polarizers (Fig. 7b). The fluid material showed a homogeneous green–yellow luminescence, which is typical of naphthalene moieties (Fig. 7c). It should be noted that the compound was still luminescent at elevated temperatures. Despite the formation of well-defined textures with compound **11**, no domains with different emissions have been observed at the present stage.

## Conclusion

Our results show that grafting of trialkoxybenzamide residues to carbazole or naphthalene skeletons induces liquid crystalline properties. The nature of the group linking the flat core to the gallate fragment plays a crucial role in the stabilization of the thermotropic mesophases. The length of the aliphatic chains has a small effect on the LC temperature range. A decrease of about 30 °C was found by increasing a single chain length from 12 to 16 carbons. The liquid crystalline properties of the carbazole family are sensitive to the presence of substituents on the nitrogen atom present at the tip of the five member ring. In contrast, compounds of the naphthalene series are more tolerant to structural chemical transformations, such as the grafting of an ester, an acid or even of an amide function, and consequently LC properties are not significantly altered, providing columnar phases with various lattice symmetries. Interestingly, a dyad, prepared by connecting a naphthalene template to a carbazole derivative, led to a liquid crystalline compound over a temperature range of about 80 °C. These novel compounds are prone to aggregation in solution but also in the solid state as scrutinized

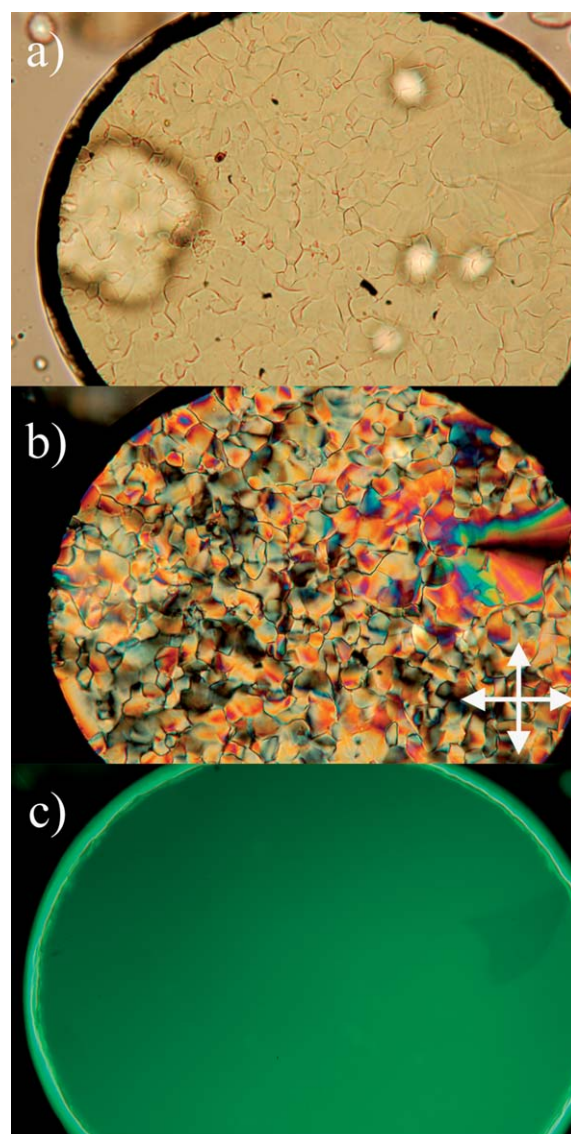


Fig. 7 Drop of compound **11** observed by optical microscopy at 180 °C: a) with a white light in transmission; b) with a white light in transmission between crossed-polarizers (symbolized by the cross in the corner of the picture) (classical texture); c) upon irradiation at  $300 < \lambda_{\text{ex}} < 350$  nm.

by absorption and fluorescence studies. Luminescent aggregates are also observed in the mesophase. In all cases, the amide functions are engaged in a supramolecular hydrogen-bonded network, as confirmed by infra-red studies. This work demonstrates guidelines for programming fluorescent ligands into self-assembled structures. Such dyads might be suitable for applications in organic devices since electron rich and electron poor molecules need to be assembled into nano-segregated structures for efficient charge separation and charge transport.<sup>38</sup> Current work along these lines is in progress in our laboratory.

## Notes and references

- (a) W. Lu, Y. Chen, V. A. L. Roy, S. S.-Y. Chui and C.-M. Che, *Angew. Chem., Int. Ed.*, 2009, **48**, 7621–7625; (b) J. W. Chung, S.-J. Yoon, S.-J. Lim, B.-K. An and S. Y. Park, *Angew. Chem., Int. Ed.*, 2009, **48**, 7030–7034; (c) K. Okano, Y. Mikami and

- T. Yamashita, *Adv. Funct. Mater.*, 2009, **19**, 3804–3808; (d) S. Yagai, T. Kinoshita, Y. Kikkawa, T. Karatsu, A. Kitamura, Y. Honsho and S. Seki, *Chem.—Eur. J.*, 2009, **15**, 9320–9324; (e) S.-I. Noro, R. Tsunashima, Y. Kamiya, K. Uemura, H. Kita, L. Cronin, T. Akutagawa and T. Nakamura, *Angew. Chem., Int. Ed.*, 2009, **48**, 8703–8706; (f) Y. Sagara, S. Yamane, T. Mutai, K. Araki and T. Kato, *Adv. Funct. Mater.*, 2009, **19**, 1869–1875; (g) A. Marrocchi, M. Seri, C. Kim, A. Facchetti, A. Taticchi and T. J. Marks, *Chem. Mater.*, 2009, **21**, 2592–2594; (h) A. Wicklein, A. Lang, M. Muth and M. Thelakkat, *J. Am. Chem. Soc.*, 2009, **131**, 14442–14453; (i) T. Yasuda, H. Ooi, J. Morita, Y. Akama, K. minoura, M. Funahashi, T. Shimomura and T. Kato, *Adv. Funct. Mater.*, 2009, **19**, 411–419; (j) R. Abbel, R. van der Weegen, W. Pisula, M. Surin, P. Leclère, R. Lazzaroni, E. W. Meijer and A. P. H. J. Schenning, *Chem.—Eur. J.*, 2009, **15**, 9737–9746; (k) A. C. Benniston, A. Harriman, D. B. Rewinska, S. Yang and Y.-G. Zhi, *Chem.—Eur. J.*, 2007, **13**, 10194–10203; (l) L. A. Lucas, D. M. Delongchamp, L. J. Richter, R. J. Kline, D. A. Fischer, B. R. Kaafarani and G. E. Jabbour, *Chem. Mater.*, 2008, **20**, 5743–5749; (m) S. Zhang, Y. Guo, L. Wang, Q. Li, K. Zheng, X. Zhan, Y. Liu, R. Liu and L.-J. Wan, *J. Phys. Chem. C*, 2009, **113**, 16232–16237.
- 2 (a) J.-M Lehn, *Supramolecular Chemistry*, VCH, Weinheim, 1995; (b) D. L. Caulder and K. N. Raymond, *Acc. Chem. Res.*, 1999, **32**, 975–982; (c) M. Fujita, K. Umemoto, M. Yoshizawa, N. Fujita, T. Kusakawa and K. Biradha, *Chem. Commun.*, 2001, 509–518; (d) A. R. Hirst, B. Escuder, J. F. Miravet and D. K. Smith, *Angew. Chem., Int. Ed.*, 2008, **47**, 8002–8018.
- 3 T. Kato, N. Mizoshita and K. Kishimoto, *Angew. Chem., Int. Ed.*, 2006, **45**, 38–68.
- 4 (a) S. Laschat, A. Baro, N. Steinke, F. Giesselmann, C. Hägele, G. Scalia, R. Judele, E. Kapatsina, S. Sauer, A. Schreivogel and M. Tosoni, *Angew. Chem., Int. Ed.*, 2007, **46**, 4832–4887; (b) S. Sergeev, W. Pisula and Y. H. Geerts, *Chem. Soc. Rev.*, 2007, **36**, 1902–1929; (c) Y. Shimizu, K. Oikawa, K.-I. Nakayama and D. Guillon, *J. Mater. Chem.*, 2007, **17**, 4223; (d) S. Kumar, *Chem. Soc. Rev.*, 2006, **35**, 83–109.
- 5 (a) A. M. van de Craats, N. Stutzmann, O. Bunk, N. N. Nielsen, M. Watson, K. Müllen, H. D. Chanzy, H. Sirringhaus and R. H. Friend, *Adv. Mater.*, 2003, **15**, 495–499; (b) W. Pisula, A. Menon, M. Stepputat, I. Lieberwirth, U. Kolb, A. Tracz, H. Sirringhaus, T. Pakula and K. Müllen, *Adv. Mater.*, 2005, **17**, 684–689; (c) T. Kitamura, S. Nakaso, N. Mizoshita, Y. Tochigi, T. Shimomura, M. Moriyama, K. Ito and T. Kato, *J. Am. Chem. Soc.*, 2005, **127**, 14769–14775; (d) J.-P. Hong, M.-C. Um, S.-R. Nam, J.-I. Hong and S. Lee, *Chem. Commun.*, 2009, 310–312; (e) S. Allard, M. Forster, B. Souharce, H. Thiem and U. Scherf, *Angew. Chem., Int. Ed.*, 2008, **47**, 4070–4098; (f) M. Mas-Torrent and C. Rovira, *Chem. Soc. Rev.*, 2008, **37**, 827–838.
- 6 (a) U. Mitschke and P. Bäuerle, *J. Mater. Chem.*, 2000, **10**, 1471–1507; (b) T. Hassheider, S. A. Benning, H.-S. Kitzerow, M.-F. Achard and H. Bock, *Angew. Chem., Int. Ed.*, 2001, **40**, 2060–2063.
- 7 (a) M. A. Loi, E. Da Como, R. Zamboni and M. Muccini, *Synth. Met.*, 2003, **139**, 687–690; (b) M. A. Loi, E. Da Como, F. Dinelli, M. Murgia, R. Zamboni, F. Biscarini and M. Muccini, *Nat. Mater.*, 2005, **4**, 81–85.
- 8 (a) B. A. Gregg, M. A. Fox and A. J. Bard, *J. Phys. Chem.*, 1990, **94**, 1586–1598; (b) A. M. Fox, J. V. Grant, D. Melamed, T. Torimoto, C.-Y. Liu and A. J. Bard, *Chem. Mater.*, 1998, **10**, 1771–1776; (c) L. Schmidt-Mende, A. Fechtenkötter, K. Müllen, E. Moons, R. H. Friend and J. D. MacKenzie, *Science*, 2001, **293**, 1119–1122; (d) W. Kubo, S. Kambe, S. Nakade, T. Kitamura, K. Hanabusa, Y. Wada and S. Yanagida, *J. Phys. Chem. B*, 2003, **107**, 4374–4381.
- 9 (a) P. Terech and R. G. Weiss, *Chem. Rev.*, 1997, **97**, 3133–3159; (b) L. A. Estroff and A. D. Hamilton, *Chem. Rev.*, 2004, **104**, 1201–1217; (c) N. M. Sangeetha and U. Maitra, *Chem. Soc. Rev.*, 2005, **34**, 821–836; (d) R. G. Weiss and P. Terech, *Molecular Gels, Materials With Self-Assembled Fibrillar Networks*, Springer, Dordrecht, 2006.
- 10 F. Camerel, G. Ulrich and R. Ziessel, *Org. Lett.*, 2004, **6**, 4171–4174.
- 11 R. Ziessel, G. Pickaert, F. Camerel, B. Donnio, D. Guillon, M. Cesario and T. Prange, *J. Am. Chem. Soc.*, 2004, **126**, 12403–12413.
- 12 R. Ziessel, F. Camerel and B. Donnio, *Chem. Rec.*, 2009, **9**, 1–23.
- 13 (a) F. Camerel, L. Bonardi, M. Schmutz and R. Ziessel, *J. Am. Chem. Soc.*, 2006, **128**, 4548–4549; (b) F. Camerel, L. Bonardi, G. Ulrich, L. Charbonnière, B. Donnio, C. Bourgogne, D. Guillon, P. Retailleau and R. Ziessel, *Chem. Mater.*, 2006, **18**, 5009–5021.
- 14 F. Camerel, R. Ziessel, B. Donnio, C. Bourgogne, D. Guillon, M. Schmutz, C. Iacovita and J.-P. Bucher, *Angew. Chem., Int. Ed.*, 2007, **46**, 2659–2662.
- 15 F. Camerel, R. Ziessel, B. Donnio and D. Guillon, *New J. Chem.*, 2006, **30**, 135–139.
- 16 (a) R. M. Adhikari, L. Duan, L. Hou, Y. Qiu, D. C. Neckers and B. K. Shah, *Chem. Mater.*, 2009, **21**, 4638–4644; (b) J. Ding, B. Zhang, J. Lu, Z. Xie, L. Wang, X. Jing and F. Wang, *Adv. Mater.*, 2009, **21**, 4983–4986; (c) M. Melucci, L. Favaretto, C. Bettini, M. Gazzano, N. Camaioni, P. Maccagnani, P. Ostojca, M. Monari and G. Barbarella, *Chem.—Eur. J.*, 2007, **13**, 10046–10054.
- 17 (a) J. S. Park, M. Song, S.-H. Jin, J. W. Lee, C. W. Lee and Y.-S. Gal, *Macromol. Chem. Phys.*, 2009, **210**, 1572–1578; (b) T. Hiejima, Y. Takamizawa, Y. Tanaka, K. Ueda and T. Uchida, *J. Polym. Sci., Part B: Polym. Phys.*, 2010, **48**, 496–502; (c) L. Akcelrud, *Prog. Polym. Sci.*, 2003, **28**, 875–962.
- 18 (a) H. Yang, T. Yi, Z. Zhou, Y. Zhou, J. Wu, M. Xu, F. Li and C. Huang, *Langmuir*, 2007, **23**, 8224–8230; (b) H. D. P. Ali, P. E. Kruger and T. Gunnlaugsson, *New J. Chem.*, 2008, **32**, 1153–1161.
- 19 (a) S. Girouard, M.-H. Houle, A. Grandbois, J. W. Keillor and S. W. Michnick, *J. Am. Chem. Soc.*, 2005, **127**, 559–566; (b) M. K. Froemming and D. Sames, *J. Am. Chem. Soc.*, 2007, **129**, 14518–14522.
- 20 (a) B. X. Mi, Z. Q. Gao, K. W. Cheah and C. H. Chen, *Appl. Phys. Lett.*, 2009, **94**, 073507; (b) S. O. Jung, W. Yuan, J. U. Ju, S. Zhang, Y. H. Kim, J. T. Je and S. K. Kwon, *Mol. Cryst. Liq. Cryst.*, 2009, **514**, 45–54; (c) Y. Wang, X. Zhang, B. Han, J. Peng, S. Hou, Y. Huang, H. Sun, M. Xie and Z. Lu, *Dyes Pigm.*, 2010, **86**, 190–196; (d) J. Liu, Y. Wang, G. Lei, J. Peng, Y. Huang, Y. Cao, M. Xie, X. Pu and Z. Lu, *J. Mater. Chem.*, 2009, **19**, 7753–7758; (e) H.-J. Kim, J.-Y. Jin, Y.-S. Lee, S.-H. Lee and C.-H. Hong, *Chem. Phys. Lett.*, 2006, **431**, 341–345.
- 21 (a) M. J. Sienkowska, H. Monobe, P. Kaszynski and Y. Shimizu, *J. Mater. Chem.*, 2007, **17**, 1392–1398; (b) K. J. Donovan, K. Scott, M. Somerton, J. Preece and M. Manickam, *Chem. Phys.*, 2006, **322**, 471–476.
- 22 F. Camerel, B. Donnio, C. Bourgogne, M. Schmutz, D. Guillon, P. Davidson and R. Ziessel, *Chem.—Eur. J.*, 2006, **12**, 4261–4274.
- 23 J. P. Chen and A. Natansohn, *Macromolecules*, 1999, **32**, 3171–3177.
- 24 S. Girouard, M.-H. Houle, A. Grandbois, J. W. Keillor and S. W. Michnick, *J. Am. Chem. Soc.*, 2005, **127**, 559–566.
- 25 J. H. Olivier, F. Camerel, R. Ziessel, P. Retailleau, J. Amadou and C. Pham-Huu, *New J. Chem.*, 2008, **32**, 920–924.
- 26 J. Olmsted, *J. Phys. Chem.*, 1979, **83**, 2581–2584.
- 27 L. Bonardi, H. Kanaan, F. Camerel, P. Jolinat, P. Retailleau and R. Ziessel, *Adv. Funct. Mater.*, 2008, **18**, 401–413.
- 28 R. Ziessel, L. Bonardi, P. Retailleau and G. Ulrich, *J. Org. Chem.*, 2006, **71**, 3093–3102.
- 29 (a) I. A. Levitsky, K. Kishikawa, S. H. Eichhorn and T. M. Swager, *J. Am. Chem. Soc.*, 2000, **122**, 2474–2479; (b) E. Terazzi, S. Torelli, G. Bernardinelli, J.-P. Rivera, J.-M. Bénéch, C. Bourgogne, B. Donnio, D. Guillon, D. Imbert, J.-C. G. Bünzli, A. Pinto, D. Jeannerat and C. Piguet, *J. Am. Chem. Soc.*, 2005, **127**, 888–903; (c) J. Matraszek, J. Mieczkowski, D. Pocięcha, E. Gorecka, B. Donnio and D. Guillon, *Chem.—Eur. J.*, 2007, **13**, 3377–3385; (d) E. Terazzi, L. Guénée, P.-Y. Morgantini, G. Bernardinelli, B. Donnio, D. Guillon and C. Piguet, *Chem.—Eur. J.*, 2007, **13**, 1674–1691; (e) S. Qu, F. Li, H. Wang, B. Bai, C. Xu, L. Zhao, B. Long and M. Li, *Chem. Mater.*, 2007, **19**, 4839–4846; (f) C. F. He, G. J. Richards, S. M. Kelly, A. E. A. Contoret and M. O'Neill, *Liq. Cryst.*, 2007, **34**, 1249–1267; (g) C. V. Yelamagad, G. Shanker, R. V. R. Rao, D. S. S. Rao, S. K. Prasad and V. V. S. Babu, *Chem.—Eur. J.*, 2008, **14**, 10462–10471; (h) X. Li, A. Liu, S. Xun, W. Qiao, X. Wan and Z. Y. Wang, *Org. Lett.*, 2008, **10**, 3785–3787; (i) J. Han, X.-Y. Chang, L.-R. Zhu, M.-L. Pang, J.-B. Meng, S. S.-Y. Chui, S.-W. Lai and V. A. L. Roy, *Chem.—Asian J.*, 2009, **4**, 1099–1107.
- 30 F. Morale, R. W. Date, D. Guillon, D. W. Bruce, R. L. Finn, C. Wilson, A. J. Blake, M. Schröder and B. Donnio, *Chem.—Eur. J.*, 2003, **9**, 2484–2501.

- 31 (a) T. Kato, T. Kutsuna, K. Hanabusa and M. Ukon, *Adv. Mater.*, 1998, **10**, 606–608; (b) K. Hanabusa, C. Koto, M. Kimura, H. Shirai and A. Kakehi, *Chem. Lett.*, 1997, 429–430; (c) R. M. Silverstein, G. C. Bassler and T. C. Morrill, *Spectrometric Identification of Organic compounds*, 3rd edn, Wiley, 1976.
- 32 M. J. Hostetler, J. J. Stokes and R. W. Murray, *Langmuir*, 1996, **12**, 3604–3612.
- 33 S.-H. Park and C. E. Lee, *Chem. Mater.*, 2006, **18**, 981–987.
- 34 S. Zapotoczny, M. Rymarczyk-Machal, A. Stradomska, P. Petelenz and M. Nowakowska, *J. Phys. Chem. B*, 2007, **111**, 10088–10094.
- 35 J. R. Lakowicz, *Principles of Fluorescence Spectroscopy*, 3rd edn, Springer, Heidelberg, 2006.
- 36 (a) A. Bayer, J. Hübner, J. Hopitzke, M. Oestreich, W. Rühle and J. H. Wendorff, *J. Phys. Chem. B*, 2001, **105**, 4596–4602; (b) R. E. Hughes, S. P. Hart, D. A. Smith, B. Movaghar, R. J. Bushby and N. Boden, *J. Phys. Chem.*, 2002, **106**, 6638–6645.
- 37 (a) F. Camerel, G. Ulrich, J. Barbera and R. Ziessel, *Chem.—Eur. J.*, 2007, **13**, 2189–2200; (b) S. Diring, F. Camerel, B. Donnio, T. Dintzer, S. Toffanin, R. Capelli, M. Muccini and R. Ziessel, *J. Am. Chem. Soc.*, 2009, **131**, 18177–18185.
- 38 (a) J. M. Mativetsky, M. Kastler, R. C. Savage, D. Gentilini, M. Palma, W. Pisula, K. Müllen and P. Samori, *Adv. Funct. Mater.*, 2009, **19**, 2486–2494; (b) T. L. Benanti, P. Saejueng and D. Venkataraman, *Chem. Commun.*, 2007, 692–694.